Cell Adhesion Chromatography System for Biophysical to Biochemical Analysis of Human Colon Cancer Metastasis through the Vasculature

A Masters Thesis
Presented to
The Academic Faculty

by

Jaeho Oh

In Partial Fulfillment
of the Requirements for the Degree
Masters of Science in the
School of Mechanical Engineering

Georgia Institute of Technology

August 2014

Cell Adhesion Chromatography System for Biophysical to Biochemical Analysis of Human Colon Cancer Metastasis through the Vasculature

Approved by:

Dr. Susan N. Thomas, Advisor
School of Mechanical Engineering
Georgia Institute of Technology

Dr. J. Brandon Dixon
School of Mechanical Engineering
Georgia Institute of Technology

Dr. Todd Sulchek
School of Mechanical Engineering
Georgia Institute of Technology

Date Approved: June 30, 2014

DEDICATION

To my wife and daughter,

Sujin Kim, Suah Oh

To my family,

Yongtaik Oh, Kwangju Kim, Joungmin Oh

To my parents in law,

Chusang Kim, Soojung Kang

ACKNOWLEDGMENTS

I would like to thank Dr. Susan N. Thomas for her time, ideas, and efforts to create and improve this thesis. This work was possible due to her enthusiasm towards the research and great advising. She helped me to learn the skills and techniques required to successfully pursue the study presented in this paper.

I would like to thank Dr. Donnell for his comments and suggestions on my thesis as well as encouragement to improve the quality of writing.

I greatly appreciate my previous co-worker, Mason Mcclatchey, who participated in this project and developed a novel program that was used in part for analyzing the data.

I would like also to thank my wife, Sujin Kim, for supporting me mentally and physically in completing this thesis. I am thankful to my family members, Yongtaik Oh, Kwangju Kim, Chusang Kim, Soojung Kang, Joungmin Oh, Heejin Kim, and David Sutton, whose support and strong belief in me have helped me to overcome hardships and devote myself to the study.

TABLE OF CONTENTS

LIST OF TABLES

LIST OF FIGURES

LIST OF ABBREVIATIONS

EGF	Epidermal Growth Factor
TNF	Tumor Necrosis Factor
IN	Interleukin
NF	Nuclear Factor
AP	Activator Protein
sLe^x	Sialyl-Lewis x
sLe^a	Sialyl-Lewis a
PSGL	P-selectin Glycoprotein Ligand
HEV	High Endothelial Venule
PCLP	Podocalyxin-like Glycoprotein
AFM	Atomic Force Microscopy
BFP	Biomembrane Force Probe
PPFC	Parallel Plate Flow Chamber
PMMA	Polymethlmethacrylate
PDMS	Polydimethylsiloxane
DPBS	Dulbecco's Phosphate-buffered Saline
EDTA	Ethylenediaminetetraacetic Acid
RTD	Residence Time Distribution
SF	Settling Feature
CDF	Cummulative Distribution Fuction

SUMMARY

Circulating cell adhesion amidst the high shear environment of the vasculature is central to several physiological and pathophysiological processes, including leukocyte recruitment to sites of inflammation, stem cell homing and cancer metastasis. This process is initiated by selectin-mediated adhesion, the molecular "brakes" that slow cells down relative to bulk fluid flow to facilitate cell-cell signaling and eventual firm cell adhesion. Selectin recognition therefore represents a critical step whereby therapeutic interventions aimed towards the interference of cell homing could be targeted. While the force dependency of these high k_{on} and k_{off} rate interactions has been well described, little understanding exists of the long time- and length-scale interactions of different cell subtypes that would best describe the functional capacity of different cell homing via selectins to systemic peripheral tissues. This limits the adequate description of sustained cell adhesion efficiencies in physiological conditions that predicates the effectiveness of cell homing as well as the design effective therapeutic interventions to selectively attenuate metastasis but not normal cell homing using such criteria. To address this issue, we developed a so-called "cell adhesion chromatography" system, a microfluidic-based device designed for use in conjunction with videomicroscopy for the interrogation of the adhesion behavior of cells over long time- and length-scales. In order to achieve uniform contact of a pulse cell suspension input into a selectin-functionalized parallel plate flow chamber, we designed a feature that enables complete cell settling to the chamber bottom based on Stoke's flow predictions, increasing contact uniformity of the pulse cell input with the substrate upon entry into the main chromatography channel from ~50 to >95%. Using this configuration, residence time distributions for a pulse input of cells perfused at defined shear stresses were generated based on cell elution times from the cell adhesion

chromatography system. Selectin-functionalized substrates delayed cell elution times relative to bovine serum albumin coated-substrates by orders of magnitude in a selectin concentration, shear and cation dependent fashion. Preliminary experiments were also performed to begin to define the differences in efficiencies of healthy (human monocyte) versus malignant (human colon carcinoma) cell adhesion to selectins in shear flow. Our results suggest significant differences in the functional capacity of healthy versus malignant cells to sustain adhesion in shear flow and that cell adhesion chromatography is a new tool that provides unique insight into the process of cell adhesion in fluid flow.

CHAPTER 1

INTRODUCTION

This chapter provides background information to help readers better understand the study presented in Chapter 4. It begins with descriptions of physiological and pathophysiological cell adhesion in the vasculature and then introduces relevant biomolecules involved in these processes. A description of experimental tools commonly employed in the aforementioned studies is also discussed.

1.1 Overview of Cell Adhesion in the Circulatory System

1.1.1 Cell Adhesion in Physiological and Pathophysiological Conditions

Circulating cell adhesion to the vascular endothelium is central to several physiological and pathophysiological processes, including leukocyte recruitment to sites of inflammation, stem cell homing and metastasis. As one example, leukocyte homing to sites of injury is a first line of physiological protection system against pathogens. Leukocytes flowing in the bloodstream move to the injured tissue upon sensing the chemical cues released from the damaged tissue. As they approach the sites, they interact with the inflamed endothelium and eventually migrate into where they fight pathogens. In a pathophysiological scenario, cancer cells are able to metastasize by overcoming shear forces from blood flow to interact with the vascular endothelium that facilitates the eventual invasion of metastatic cells into peripheral tissues to establish secondary tumors. This process of adhesion, crucial to the aforementioned diverse physiological phenomena, is multistep, including cell tethering or rolling over the endothelial layer, conversion of these transient interactions to firm adhesion, and eventual cell transmigration through the endothelial cell layer. Selectins and their ligands provide the initial brakes that slow cells down relative to bulk fluid

flow, and are characterized by tethering and/or rolling interactions. In response to chemokine- or non-chemokine-mediated signaling, other cell adhesion molecule receptor-ligand bonds can form with increased cell-cell contact times or alternatively the affinity of integrins on the cell surface is enhanced [1,2], which converts cell rolling interactions to firm adhesion. Subsequently, these cells can then transmigrate through the endothelial cell-cell junctions to infiltrate the site of infection or damaged tissue.

1.1.2 Hemodynamic Forces in the Vasculature

In the circulatory system, hemodynamic forces result from blood flow. The magnitude of shear force depends on the locations within the circulatory system due to a varying blood vessel diameter and local vascular diseases. For example, shear stress is about 10 dyn/cm^2 in arterioles, and it varies from 1 to 5 dyn/cm^2 in venules for humans [3]. Vascular diseases, such as atherosclerosis, can impact local wall shear stress levels considerably. It has been reported that the shear stress in vascular bifurcations, such as carotid, coronary, renal, and iliac artery flow divisions, that have atherosclerotic lesions was on the order of 4 dyn/cm^2, whereas it was about 12 dyn/cm^2 at disease-free regions [4]. Such variations in the hemodynamic microenvironment play a role in precisely regulating the extent and dynamics of cell adhesion. For instance, flow-enhanced leukocyte adhesion was evidenced by Yago [5]. Interestingly, similar flow-enhanced adhesion was also seen from the interactions between bacteria and red blood cells [6]. These findings explain the tight relationship between the precise hemodynamic microenvironment and the physiological homing behavior observed in *in vivo* systems.

1.2 Cell Adhesion Molecules

1.2.1 Selectins

Selectins are a family of transmembrane glycoproteins that bind carbohydrate moieties expressed by their ligands on the surfaces of apposing cells. They include P-, L-, and E-selectin [7]. The names of the selectins originate from platelet, leukocyte, and endothelium for P-, L-, and E-selectin, respectively. The structures of the selectins are similar; they all consist of an extracellular C-type lectin domain, an EGF (Epidermal Growth Factor) domain, variable numbers (2, 6, and 9 for L-, E-, and P-selectin, respectively) of short consensus repeats domains, a transmembrane domain, and a cytoplasmic tail [7,8], which can be seen in Figure 1.2.1.

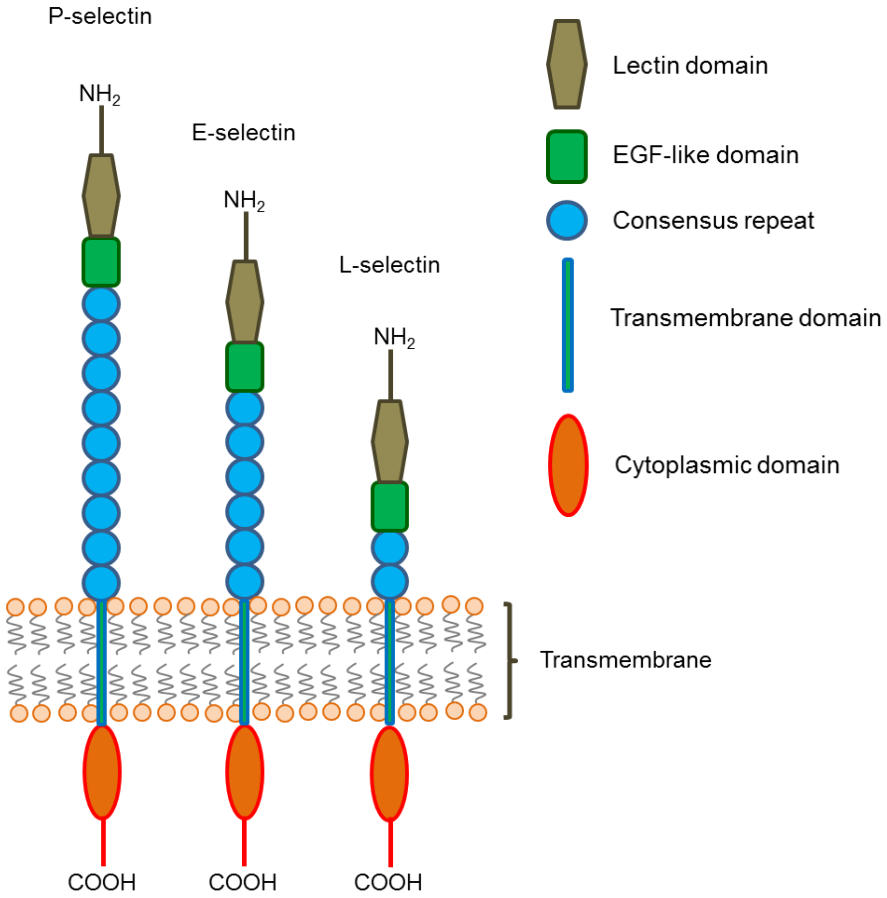

Figure 1.2.1 Schematic of selectin molecular structure. The selectin family of receptors share C-type lectin, EGF-like, transmembrane, and cytoplasmic domains. Each type has a different number of consensus repeats (9, 6, and 2 for P-, E-, and L-selectin, respectively). Reproduced from Gahmberg et al. 1999 [9].

P-selectin is constitutively expressed in Weibel-Palade bodies in the endothelium and in secretory granules (alpha-granules) in platelets [10]. Then, P-selectin can be rapidly expressed on a plasma membrane upon stimulation by histamine and thrombin generated at the site of injury [11]. P-selectin can interact with its ligands on platelets, leukocytes, and a number of cancer cells [12]. For example, interactions between leukocytes and platelets are mediated by P-selectin on platelets and its ligand, PSGL-1, on leukocytes, and it promotes fibrin deposition at the site of injury [13]. Human breast carcinoma cells, K9, expressing CD24, a GPI-linked surface mucin, showed binding activity to P-selectin under flow condtions [14]. L-selectin is expressed on the surface of leukocytes and contributes to leukocyte trafficking to the site of inflamed endothelium in the circulatory system [15]. Cancer cells can also bind to L-selectin on the surface of leukocytes, which can either discourage or promote metastasis to a remote location [16]. E-selectin is expressed by endothelial cells, but not constitutively. It is transcriptionally regulated in response to several transcription factors such as tumor necrosis factor α (TNFα), interleukin (IL)-1, nuclear factor κB (NF-κB), and activator protein 1 (AP-1) [17]. E-selectin can bind to glycosphingolipids expressed on human neutrophils [18] as well as L-selectin [7] on the surface of leukocytes.

1.2.2 Selectin Ligands

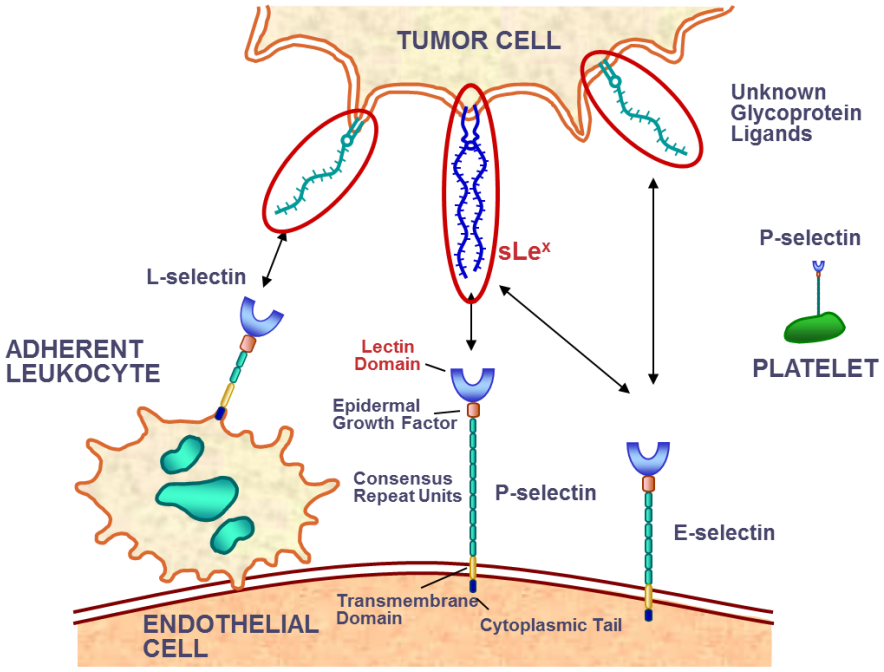

Figure 1.2.2 Schematic of selectin-ligand binding. The schematic shows a circulating tumor cell interacting with host cells via interactions between seletins and their ligands. A blood-borne tumor cell can interact with endothelial cells by recognition between sialofucosylated ligands with P- and/or E-selectin. They may also interact with leukocytes and platelets via sialofucosylated ligands recognition by L-selectin and P-selectin, respectively. Reproduced from Konstantopoulos and Thomas, 2009 [7].

1.2.2.1 Selectin-binding Glycans

Selectins recognize glycans via their C-type lectin domains [7]. There are three types of carbohydrate structures to which selectins can bind oligosaccharides, phosphorylated mono- and polysaccharides and sulfated polysaccharides [19]. One of the major binding determinants of all three selectin types is tetrasaccharide sialyl-Lewis x (sLe^x) and its isomer sialyl-Lewis (sLe^a) , which is affiliated with oligosaccharides [20]. However, each selectin shows different characteristic binding

to its ligands depending on the ligand structure. L-selectin binds with high affinity to glycoproteins with O-linked glycans in which the sLe^x determinant is present, whereas E-selectin binds with relatively high affinity to sialylated polyfucosylated N-linked glycans [7]. E- and P-selectin also bind to O-linked glycans [21].

1.2.2.2 Selectin-binding Glycoproteins

The selectin family can recognize tetrasaccharide sLe^x and sLe^a, a structural isomer of sLe^x, as mentioned above. Determinants recognized by the selectin family are typically found as terminal residues of larger oligosaccharides on glycoproteins [19]. Many selectin-binding glycoproteins have been identified and a few examples are discussed here. First, P-selectin Glycoprotein Ligand-1 (PSGL-1) is recognized as the major binding ligand of all three selectin types. PSGL-1 is constitutively expressed on all leukocytes and plays an important role in inflammation by allowing immune cells to bind to the activated endothelium that expresses P-selectin and to reach the site of inflammation [22]. PSGL-1 also recognizes L- and E-selectin, but these interactions require different post-translational modifications on PSGL-1 than the ones for binding to P-selectin; L-selectin recognizes NH_2 terminal domain that possesses tyrosine sulfate and O-glycans, and E-selectin binds to PSGL-1with Core-2, sialylated and fucosylated O-glycans [23]. PSGL-1 participates in interactions between leukocytes and E-selectin-expressing endothelium as well as between neutrophil-neutrophil interactions [24]. CD34 is a heavily glycosylated type I transmembrane protein that is expressed on high endothelial venule (HEV) and serves as a ligand for L-selectin [25]. For example, a lymphocyte binding to HEVs is mediated by L-selectin and its ligand, CD34, on the surface of the lymphocyte and HEV, respectively. However, CD34 needs to be modified through sialylation, fucosylation, and sulfation for elaborated adhesion to L-selectin [26]. Next, CD44 is a class I transmembrane glycoprotein that is present on leukocytes and

endothelial cells. CD44 found on neutrophils was identified as an E-selectin ligand, whereas CD44 expressed on different cell types (bone marrow stromal cells and brain endothelial cells) did not show binding activity to E-selectin, suggesting that there exist different posttranslational modifications between CD44's on different cell types [27]. In order for CD44 to act as an E-selectin ligand, its determinant on N-linked glycans needs to be richly decorated with sialyl and fucosyl groups [28].

1.2.2.3 Selectin Ligands Expressed by Metastatic Colon Cancer Cells

A common feature of cell surface carbohydrates of all kinds of cancer cells comes from aberrant glycosylation, which differ from those on the surface of their progenitor cells [29]. Some of the aberrantly glycosylated glycoproteins on colon cancer cells that are recognized by selectins are variant isoforms of CD44 (CD44v), podocalyxin-like glycoprotein (PCLP), death receptor-3 (DR3), and carcinoembryonic antigen (CEA). CD44v is a class of isoforms of CD44 formed due to extracellular domain exon splicing [7]. A study by Hanley revealed a function of O-linked glycans on CD44v expressed by colon carcinoma cells (LS174T) has E-selectin ligand activity [30]. Later work indicated its function as a L- and P-selectin ligand as well [31,32]. The up-regulation of CD44v is closely associated with a pathophysiological condition such as cancer metastasis, and results in poor prognosis [33]. PCLP is a transmembrane glycoprotein that is a part of the CD34 family. PCLP has been recognized as a marker for kidney glomerular epithelial cells (podocytes) [34] and it participates in kidney development. Alterations in the heavily charged sialomucin was found to be related to nephrotic syndrome, which compensates for the function of podocytes as filters in kidney [35]. PCLP is also expressed on vascular endothelial cells, hematopoietic stem cells, and progenitor cells [34]. A recent study also identified PCLP on colon cancer cells, and it was found to function as ligand for E- and L-selectin, but not as P-selectin [36]. A clinical study found that the overexpression

of PCLP on colon cancer cells was an indication of potential metastatic activity [37]. PCLP was also present on the surface of other cancer types, such as breast [38] and pancreas [39]. Death Receptor-3 (DR3), also alternatively named Ws1, Apo3, TRAMP, LARD, TR3, or TNFRSF25, is a member of the Tumor Necrosis Factor (TNF) receptor superfamily [40]. It is expressed by some immune cells (peripheral blood leukocytes [41] and T cells [42]) and within various tissues (spleen, thymus, and brain [42]). DR3 was found to trigger apoptosis by inducing increase in DNA fragments, which is an indication of programmed cell death [43]. However, a recent study found another function of DR3, which was as an E-selectin ligand on colon cancer cells [41]. Additionally, this study demonstrated that E-selectin-bound DR3 appeared to enhance the survival rate of colon cancer cells by activating extracellular signal-regulated kinase and help migration of colon cancer cells by benefiting from p38 mitogen-activated protein kinase activity. Carcinoembryonic Antigen (CEA) has been identified to be a single heavily glycosylated protein [44] that is normally produced in the gastrointestinal tract in developing fetal digestive system [45]. Serum CEA levels are used diagnostically for colon cancer [44,46]. More recently CEA expressed by colon carcinoma cells were shown to display E- and L-selectin binding activity[32].

1.2.3 Selectin-ligand Biophysics

The biophysics of selectin-ligand interactions have been widely investigated, given the tight regulation of selectin-mediated cell adhesion by mechanical force resulting from blood flow in the vasculature. For example, leukocyte recruitment to the inflammation site involves fast selectin-ligand binding, which allows the cells to roll on the vascular endothelium. This behavior is associated with rapid k_{off} and k_{on} rates, which are influenced by bond loading [47]. The dissociation rate, k_{off}, was estimated by utilizing the Hookean spring model and the association rate, k_{on}, has been determined by employing computer simulations based on the Bell model [48,49]. The

dependency of the association rate on loading rate has been studied by Lü [50]; the k_{on} did not monotonically increase as the loading rate increased, but exhibited a biphasic behavior, where the k_{on} increased until a certain loading rate and decreased thereafter. Also, a study of how the loading influences the dissociation rate was conducted by Wayman [51]. The results demonstrated that the k_{off} followed a triphasic trend, which is realted to flow-enhanced binding between the selectin and its ligand. Usually, a larger shear stress (loading) exerts more tensile force on the bond, thus it is more subject to bond breakage, and vice versa. However, triphasic force-dependent bond behavior was observed for selectin-ligand interactions [51–53]. First, the bond lifetime decreased (increase in k_{off}) with increasing shear stress, which is known as a slip-bond. Then, within a certain range of shear stress the bond lifetime increases (decrease in k_{off}) as the shear stress increased; this is referred to as a catch-bond. Prolonged bond lifetime in this example is the consequence of hemodynamic drag, which provokes conformational changes in the lectin-EGF domain hinge of selectins in a way that promotes binding affinity between selectins and ligands [22]. After the catch-bond behavior, the bond lifetime decreases (increase in k_{off}) again with increasing shear stress, which results in a return to slip-bond behavior. These observations indicate that there may exist a threshold shear that enhances the bond lifetime between all three selectins, P-[54], L-[5], and E-selectin[55] and their ligands.

1.3 Existing Techniques to Investigate Cell Adhesion Biophysics

Various techniques have been employed to measure selectin/ligand binding biophysics. Atomic force microscopy (AFM) and biomembrane force probes (BFP) have been used to measure single molecule rate of bonding and bond lifetime between selectins and their ligands to characterize their dependence on force [51,54]. Dissociation rates resulting from various levels of flow-induced tether forces have been evaluated for selectin/ligand interactions using purified

protein and whole cell/functionalized bead flow-based adhesion assays [5]. Bond lifetime force dependencies have also been investigated using flow chamber techniques over a range of shear stresses [55].

1.3.1 Atomic Force Microscopy

AFM uses a very sensitive force probe that has a very high resolution to measure forces as low as piconewton scale, which can reveal the fundamentals of biological phenomena at molecular levels including receptor-ligand binding, cell adhesion, protein folding, etc [56]. AFM measurements are based on the deflection of a cantilever with a known spring constant. The degree of deflection is sensed by a laser reflected from the cantilever tip. Marshall et al used this technique to measure the force-dependent lifetime of bonding between P-selectin and PSGL-1 and extrapolated the dissociation rate [54]. In another study, Lü used AFM to assess the effects of contact duration, loading rate, and approaching velocity on the association rate for interactions between P-selectin and PSGL-1 [50]. These studies advanced the field's understanding of how physical forces at the piconewton scale play a role in selectin-ligand binding.

1.3.2 Biomembrane Force Probe (BFP)

The BFP technique was pioneered by E. Evans [57] and uses a principle comparable to that of AFM. The difference between BFP and AFM is the force sensor; AFM employs a cantilever beam, and BFP utilizes a cell membrane, usually red blood cells, to sense force. The advantage of BFP over AFM is that the stiffness of the cell membrane can be manipulated at the user's will by manipulating the micropipette suction pressure to hold the cell, ranging from 1 μN/m to 10 mN/m [58]. E. Evan employed a BFP to identify the chemical features involved in the transition states of binding between L-selectin and PSGL-1 by measuring forces, ranging from 1 pN to 1 nN, required to dissociate the binding between L-selectin and carbohydrates structures on PSGL-1 [59]. The

tunability and superior sensitivity of the BFP in measuring forces offers numerous advantages for the examination of biomolecular interactions.

1.3.3 Parallel Plate Flow Chamber

Parallel plate flow chambers (PPFC), used in conjunction with videomicroscopy, are widely used to investigate cell adhesion under the influence of fluid flow, as they allow researchers to create an *in vitro* platform that mimics the *in vivo* hemodynamic microenvironment. Examples of commercially available PPFCs are seen in Figure 1.3.3.1.

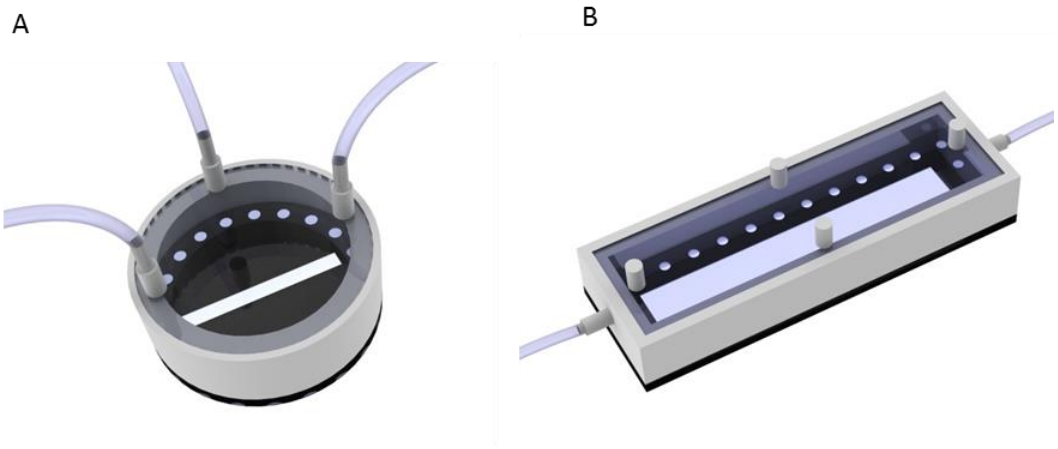

Figure 1.3.3.1. Conventional parallel plate flow chambers (PPFCs). A circular (A) and rectangular (B) PPFC are shown.

The flow regime within the PPFC is laminar with well-defined velocity profile as seen in Figure 1.3.3.2.

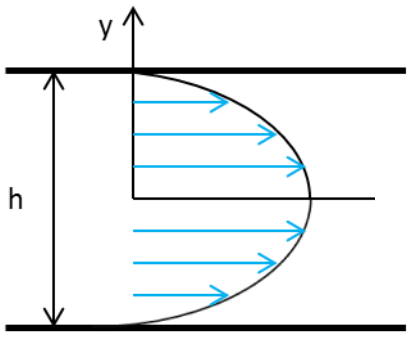

$$v_x = \frac{\tau}{h\mu_w}\left(\frac{h^2}{4} - y^2\right)$$

Figure 1.3.3.2. Laminar parabolic velocity profile and equation of PPFC. Laminar flow profile within the chamber is schematically described and the corresponding velocity profile equation is shown.

Moreover, the PPFCs are capable of producing uniform wall shear stress throughout the channel. Giavazzi utilized PPFC to study the interactions between human tumor cells (colon carcinoma, ovarian carcinoma, and breast carcinoma) and the vascular endothelium under the uniform physiological shear environment [60]. This is the most basic way to use PPFC. By modifying and adding features to the conventional PPFC devices, more complex and physiologically relevant studies can be conducted. For example, cell adhesion strength can be studied by applying fluid flow at different shear stresses. Rupprecht incorporated tapered channels of different heights to PPFC with a substrate coated with adhesion molecules to study the detachment kinetics of adhesion interactions and the shear-dependent motion in cell adhesion. The tapered channels created various shear stresses within a channel having one single flow rate; this was used to determine the shear-sensitivity of cell detachment by observation with an inverted light microscope [61]. Another example involves modification of topological cues within PPFC to study adhesive behaviors of the cells. A study by Martines adapted nanopits on the bottom of the flow chamber to observe the effects of topological features on cell adhesion in dynamic conditions [62].

A mold for the nanopatterned substrates was fabricated by means of electron beam lithography, and the mold was embossed into a sheet of solid polymethylmethacrylate (PMMA). Then, the patterned PMMA sheet was incorporated into the chamber to examine cell adhesion on the nano-topography under the laminar flow. Another study performed by Herman paid attention to the effects of biochemical cues on cell adhesion [63]. A concentration gradient of adhesion molecules was created by situating a UV-modifiable glass substrate with protein-containing solution in the presence of well-controlled UV exposure; this was to mimic the spatially varying ligand concentration in a physiological environment. This system incorporated into PPFC enabled study of cell adhesion to the ligand under the physiologically relevant shear stress.

1.4 Motivation

To date, only the instantaneous behavior of selectin-ligand binding interactions have been investigated from both a biophysical and biomechanical perspective, leaving selectin-mediated cell adhesion over long time and length scales uncharacterized. Yet the capacity of cells to sustain interactions with the vasculature during their transit through the circulatory system as mediated by E- and P-selectin influences their capacity to respond to chemokine signaling and activate firm adhesion to the endothelium. This in turn predicates whether a cell will transmigrate to take up residence in the surrounding tissue. Delineating the efficiency with which different cell types sustain interactions with selectin substrates will therefore yield new insights into how selectins may differentially regulate the cell-cell crosstalk involved in directing cell engraftment during the processes of inflammation versus metastasis. This will furthermore provide new criteria for the identification of interventions aiming to selectively attenuate one or more of these cell homing processes.

CHAPTER 2

AIMS OF THE PROJECT

Despite the force dependency of selectin-ligand interactions being well described, little understanding exists as to how different selectin-binding cell types interact over long time or length scales. A system that can uniformly subject whole cells to shear flow conditions as well as prescribed chamber lengths of selectin-functionalized substrates is thus required. By developing a microfluidic-based cell adhesion chromatography system, our aim is to elaborate on the adhesive behavior of normal versus malignant cells to selectins at the macro scale (over centimeters) for sustained times (120 minutes). As such, a so-called "cell adhesion chromatography" system is introduced in this thesis based on a parallel plate flow chamber configuration that is modified to allow cells to interact with a centimeters-long channel coated with selectins that is used in conjunction with videomicroscopy. By monitoring the individual cell elution times from a pulse cell population input, residence time distribution profiles of cells perfused in medium at physiological flow rates are generated. Our system therefore provides a simple but an innovative platform to study selectin-mediated cell adhesion in the circulatory system. This section introduces the rationale for this work. The objectives are also specifically described, including the chamber design, development of the substrate functionalization protocol, and use of this system to evaluate the adhesive behavior of normal monocytes and contrast it to that of malignant colon cancer cells.

CHAPTER 3

MATERIALS AND METHODS

3.1 COMSOL Modeling

The shear profile within the parallel plate flow chamber (PPFC) was established using COMSOL (version 4.2.1.110, COMSOL, Stockholm, Sweden). The chamber was modeled in Solidworks (version 2013 SP4.0, SOLIDWORKS, Waltham, MA) and exported as a STL file to be imported into COMSOL. After importing the chamber model into COMSOL, the fluid material was chosen to be water (liquid), and the chamber flow profile solution model set to laminar flow. The boundary walls were chosen to be the outer surface of the liquid domain, the initial velocity of the flow was set to 0 m/sec, and the location of the inlet was selected as a surface normal to the inlet circumference. The normal inflow average velocity to the inlet was set to 5.1873×10^{-5} m/sec, which was obtained by dividing a volumetric flow (in our chamber corresponds to 0.022 mL/min for a shear stress of 1 dyn/cm^2 within the main channel) by an inlet area, and the outlet of the flow was selected to be a surface normal to the outlet circumference. With all the aforementioned properties and restraints inserted, geometry meshing was performed by selecting a predefined extra fine mesh (maximum and minimum element sizes were 343 µm and 22.4 µm with maximum element growth rate to be 1.08). Once the model was solved, the shear stress profile was created by manually defining an expression for the shear stress (shear rate × dynamic viscosity); the profile was then plotted for the plane, which was distanced 2×10^{-5} µm from the chamber bottom. This position was chosen because the chamber model imported from Solidworks was located slightly off the zero coordinate of the height. Using the same simulation results, the streamline profile for

the settling feature (SF) was plotted by adding a streamline module. 100 streamline positions were defined at the inlet.

3.2 Stokes Settling Prediction

To predict the required distances for cells to settle within the flow field to the planar bottom substrate by Stokes flow, a MATLAB (ver. 12.7.0, Mathworks, Natick, MA) script was written to simulate particle trajectoryies. The parameters required to predict settling distance using Stokes' law were mass densities of the cells and of the media, dynamic viscosity of the media, the radius of the cells, gravity, and wall shear stress, which were 1.032×10^3 kg/m^3, 1.0233×10^3 kg/m^3, 9×10^{-4} Pa·sec, 14 µm, 9.81 m/sec^2, and 1.0 dyn/cm^2, respectively. The entry heights of the cells were evenly distributed over the chamber height (100 µm). A time increment of 0.1 seconds was used to obtain how far the cells settled and traveled at each time point by using Equation 2 and 3 in Section 4.1.2. Using MATLAB, the height of the cells as well as how far they traveled at each time point was stored to generate the particle trajectory until the particles reached the bottom of the chamber. The assumptions made in the calculations were that all particles were of an identical particle size and that hydrodynamic wall effects were negligible.

3.3 Chamber Fabrication

Chamber preparation for all experiments required two major parts comprising the top and the bottom of the chamber. The top part of the chamber was a polydimethylsiloxane (PDMS) block with an open channel that when bonded to a polystyrene plastic plate (Corning, Cat. #: 431111), a closed channel was formed. Briefly, the molds with a negative feature for the PDMS block were produced by micro-machining an aluminum block (Alloy 6013) with a micro-milling machine (OM 1-A, HAAS, Oxnard, CA). Silicone elastomer base and curing agent at a ratio of 9:1 was poured into the mold and cured at 90˚C for 3 to 4 hours. After the curing process, a biopsy punch

was used to make holes for an inlet and an outlet. Then, glass slides were spin-coated (WS-400BZ-6NPP-LITE, Laurell, North Wales, PA) at 6000 RPM for one minute with a mixture of PDMS elastomer base and curing agent at a ratio of 10:1. Then, the bottom of the PDMS block was stamped on the glass slides by placing the PDMS block with the surface that had the open channel facing the surface of the glass slide coated with the uncured PDMS, which functioned as glue, and gently pressing the PDMS block against the glass slide. Care was taken to ensure that no air bubbles formed at the interface between the PDMS block and the plastic plate. Then, the whole assembly was treated with heat in a 50˚C oven for 12 to 15 hours to completely cure the PDMS mixture to finalize chamber bonding. After the curing process, the chamber was cooled to room temperature and functionalization the same day.

3.4 Chamber Functionalization

The main chromatography channel of the chamber was first incubated at 4 ℃ overnight with Anti-IgG solution at the desired final selectin concentration (2.5 and 25 µg/mL) in Dulbecco's phosphate-buffered saline (DPBS) by infusing a volume of solution from the outlet sufficient to just cover the main channel. On the following day, the main channel was washed three times by injecting DPBS from the outlet to wash the main channel only, which was then blocked by adding 1% BSA from the outlet for 1 hour at room temperature. After blocking, the main channel was washed with DPBS and functionalized with selectin solution made at a desired concentration (2.5 and 25 µg/mL) in DPBS for 2 hours at room temperature, both introduced from the outlet. Then, the main channel was washed with DPBS, which was injected from the outlet, and the whole chamber was blocked by injecting 1% BSA from the inlet for 1 hour at room temperature. Finally, the whole chamber was washed by infusing 1 mL of DPBS from the inlet three times and stored at room temperature until use in same day cell adhesion experiments. When storing the

functionalized chamber, the channel was filled with DPBS so as not to dry the surface of the channel. For blank chambers, whose main channel was not functionalized with selectin, the chamber was incubated with 1% BSA overnight in 4 ˚C and washed with 1mL DPBS from the inlet three times. DPBS used in all steps of the functionalization process contained calcium and magnesium except for Anti-IgG incubation step, where DPBS without calcium and magnesium was used.

3.5 Cell Culture

The human colorectal carcinoma cell line LS174T was obtained from the American Type Culture Collection (Manassas, VA) and cultured in DMEM supplemented with 10% heat-inactivated FBS and 1% antibiotic-antimycotic. LS174T cells were passaged when they reached 90% confluency. For cell adhesion experiments, LS174T cells were harvested by mild trypsinization by using 0.25% Trypsin/EDTA for 3 minutes at 37˚C and subsequently incubated at a concentration of 10^7 cells/mL in culture media at 37˚C for 2 hours to allow regeneration of surface glycoproteins. After 2 hours of surface protein regeneration, LS174T cells were centrifuged at 300 g for 5 minutes and washed with DPBS containing calcium and magnesium. Then, the cells were centrifuged again at 300 g for 5 minutes and resuspended in 0.1 % BSA in DPBS with calcium and magnesium to achieve the final concentration of 5×10^5 cells/mL. THP-1 cells were generously provided by Dr. Cheng Zhu (Atlanta, GA) and cultured in RPMI 1640 supplemented with 10% heat-inactivated FBS, 1 mM Sodium Pyruvate, and 10 mM HEPES in suspension culture. THP-1 cells were passaged every three days with the dilution ratio of 1:4 or 1:5 depending on the cell density. THP-1 cell density was determined every date of use to ensure sure that the density was in the recommended range ($< 1 \times 10^6$ cells/mL). The preparation of THP-1 cells did not require surface glycoprotein regeneration since they were collected without

trypsinization. Therefore, they were centrifuged at 300 g for 5 minutes to wash with DPBS containing calcium and magnesium without incubating them at 37 ℃. After the washing step, there were resuspended with 0.1 % BSA in DPBS with calcium and magnesium to achieve the final concentration of $5x10^5$ cells/mL. For perfusion experiments with ethylenediaminetetraacetic acid (EDTA), cell suspensions and perfusion medium contained 5 mM EDTA.

3.6 Cell Adhesion Chromatography Experimental Setup

The experimental setup contains three major components: a chamber, a syringe pump (Havard PHD/ULTRA; Havard Apparatus, HJolliston, MA), and an optical microscope (Eclipse Ti, NIKON, Melville, NY). Other equipment includes tubing, syringes, and an inlet reservoir. The common steps taken for all experiments are the following. The chamber, installed with the inlet reservoir and the tubing connected to the outlet, was placed on the microscope. Then, the tubing from the outlet was connected to the syringe on the syringe pump via a luer-lock connection. Next, the desired imaging site was located and the chamber was fixed on the stage of the microscope. The focal plane set in advance by focusing on the bottom of the chamber and raising the focal plane 5 μm. Prepared cell suspensions were then added to the inlet reservoir (50 μL of cell suspension concentrated at 5×10^5 cells/mL: a total of 25000 cells) as a pulse before operating the syringe pump to initiate imaging. For $H_{vel}/0.5(R_x+R_y)$ experiments as discussed in the later section (section 5.1.4), nine evenly spaced locations along the channel were used to assess the velocity and extent of cell adhesion throughout the channel. Each position was imaged during perfusion for five minute for analysis. The field of view was changed between positions without stopping the pump. For residence time distribution (RTD) experiments, the imaging site was set to either 1.3 or 14 cm from the end of the SF. Two different chamber lengths (1.3 and 14 cm) were used in this work since P-, L- and E-selectin each exhibit rolling velocities that differ by orders of magnitude.

Cells rolling slowly, over E-selectin for example, would not sufficiently elute within the two hour time frame of experimentation if a 14 cm long chamber was used. Furthermore, cells with high rolling velocity interactions with the substrate, such as those typical of L-selectin, would quickly elute with insufficient resolution over the length of a 1.3 cm chamber. Video acquisition was performed using NIS-Elements (Nikon). For all the experiments the identical camera and software settings were employed. The fps was set to be 25, the exposure time was 0.281 μsec, the magnification of the object was 10×, the video size was set to be 960 pixels by 500 pixels, and the image was binned 2 × 2. Videos generated by NIS-element were saved in an avi (audio video interleaved) format for subsequent viewing and analysis.

3.7 Data Collection

The main goal of this thesis is to discuss the design of the cell adhesion chromatography system that is utilized to study time-averaged adhesive behavior of cells with selectin-functionalized substrates. In order to prove the feasibility of the system, several types of data were collected. First, perfusion experiments without selectin-functionalized substrates were performed to check the capacity of the SF to bring a population of cells in uniform contact with the substrate. To do this, the relative effectiveness of the SF was assessed by perfusing the cells from the inlet (with SF) and compared to the calculated cell distances from the substrate calculated based on free velocity when perfused from the outlet, which lacked a SF, and hence recapitulates a conventional PPFC. Second, RTD experiments were executed. Before running RTD experiments, preliminary experiments were completed to determine the appropriate video duration and imaging sites to observe adhesive behaviors of the cells since extent of cell adhesion could vary depending on a cell type, a kind of selectin, and selectin concentrations. For this purpose, LS174T and THP-1 cells were perfused over substrates functionalized with one of three different types of selectin (P-, L-

and E-selectin) at two different concentrations (2.5 or 25 µg/mL), and rolling velocities were calculated to approximate the amount of time for imaging and the locations of the imaging sites. Based on preliminary studies, two hour videos at two different locations, 1.3 and 14 cm after the SF were determined to enable capture of >90% of the cell input population based on observed average rolling velocity distributions for E- versus L- and P-selectin, respectively. During RTD experiments, the number of rolling cells at different times post initiation of perfusion (elution time) were manually counted in one minute increments.

3.8 Data Analysis

In this paper, CELL TRACKER (Appendix A) was used to process videos generated from $H_{vel}/0.5(R_x+R_y)$ experiments. Once the videos were processed, the default data for the tracked cells (velocity, aspect ratio, x_radius, y_radius, projected areas, and height) were produced and saved in a database. At user's will, these data can be exported to an excel file for further analysis or they can be used to generate plots within the program. For the purpose of analyzing and plotting data for $H_{vel}/0.5(R_x+R_y)$ experiments, the default set of data was exported to excel files. To correctly present the data, false data points were filtered out due to background and non-cellular particle detection. First, theoretically calculated velocity profiles (529 ~ 1405 µm/sec, 1058 ~ 2809 µm/sec, and 1588 ~ 4214 µm/sec for shear stress of 0.5, 1.0, and 1.5 dyn/cm^2, respectively) based on channel geometry (2 mm by 100 µm), applied shear stress (0.5, 1.0, and 1.5 dyn/cm^2), and fluid property (dynamic viscosity: 8.9 x 10^{-4} Pa·sec) were used as a reference to sort out data points sitting outside of a theoretical velocity range. Next, the projected areas for cells were considered to exclude those with exceptionally small or large areas, assuming cell diameters could vary from 10 to 40 µm. Last, the aspect ratio was considered in order to deselect data points with distorted shapes, which might have been non-viable cells, non-cellular particles, or background.

A metric of $H_{vel}/0.5(R_x+R_y)$ (a cell's vertical position from the bottom of the chamber over an effective cell radius), which indicated how close the cells are from the chamber bottom was used in this work to estimate how effective the SF was in creating uniform cell contact with the planar bottom substrate. A value of 1.0 indicates that the cell is at the bottom of the chamber. The heights of the cells relative to the bottom of the chamber were calculated by CELL TRAKCKER based on the measured velocities; CELL TRACKER used the velocity profile in Equation 3 in Section 4.1.2 to solve it for y by plugging in known (chamber height, wall shear stress, and dynamic viscosity of medium) and a measured parameter (velocity). The sum of individual cell x and y radii (R_x and R_y, respectively) was used in this ratio calculation were also recorded using CELL TRACKER.

CHAPTER 4

RESULTS

4.1 Chamber Design

4.1.1 Cell Settling Distance Requirement

A cell chromatography system developed and tested in this study required all cells to be in contact with the substrate in the main channel to observe their adhesive behavior throughout the entire channel length. This enables us to extract representative characteristics of cell adhesion over a prolonged distance for an extended time. In conventional parallel plate flow chambers, uniform cell contact with the substrate is not achieved, which is thus problematic for the purpose of this work.

In order to find the required distances for cells to settle down in the conventional PPFCs, we employed MATLAB to simulate particle trajectories in chambers with different heights (20, 50, 100, 150, 200, and 300 μm) depending on different shear stresses (0.5, 1.0, and 1.5 dyn/cm^2) (Figure 4.1.1.1).

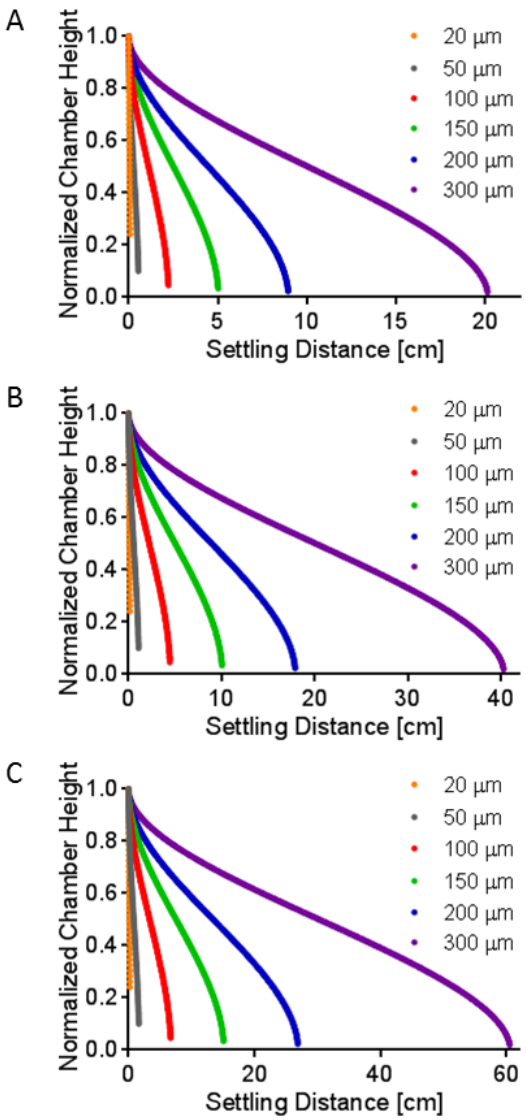

Figure 4.1.1.1 Cell settling distances for different chamber heights and shear stresses. Simulated particle trajectories within different heights of chambers (20, 50, 100, 150, 200, and 300 µm) subject to different shear stresses of 0.5, 1.0, and 1.5 dyn/cm^2 for A, B, and C, respectively.

PPFCs of conventional heights (250-300 um) do not achieve uniform cell contact with the substrate, making cell adhesion chromatography, which requires uniform contact of an entire pulse input cell population with the substrate, infeasible. Lessening the heights to enable more uniform

cell contact however requires the width of the channel to be decreased as well to prevent collapse and leads to flow through rates that are unacceptably low to yield observations for meaningful statistics. In order to generate wall shear stress of 1 dyn/cm^2 in the main channel, volumetric flow rates that can be used for the chambers with heights of 20 and 50 µm are 2.24×10^{-4} and 3.49×10^{-3} mL/min. These flow rates are not only hard to continuously generate, but also it reduces the infused pulse cell input and therefore sample size. As a compromise, we chose a chamber height of 100 µm that facilitates reasonable volumetric flow rates (0.022 mL/min for shear stress of 1 dyn/cm^2) to achieve sufficient cell throughput. However, settling of cells entering the chamber within the upper 10% of the chamber height still requires 4.5 cm of channel length. More critically, the input cell population will interact with the substrate for dramatically different lengths of time based on their height of entry, adding a large amount of undesirable variability to the data.

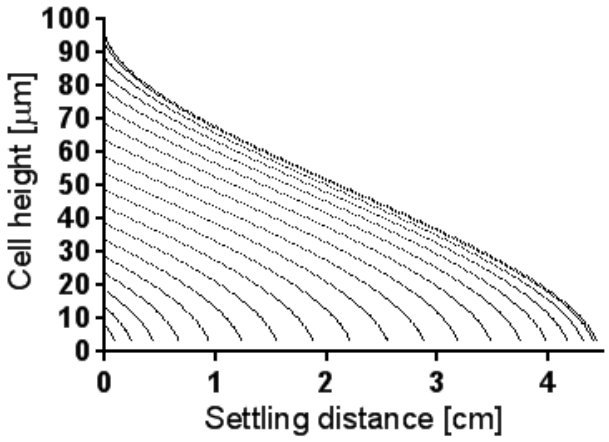

Figure 4.1.1.2 Stokes settling prediction. Simulated particle trajectories based on Stoke's settling. The cells were evenly distributed over the height of the chamber. The shear stress used for the simulation was 1 dyn/cm^2.

4.1.2 Settling Feature (SF) Design

To circumvent the undesirable heterogeneous lengths over which cells will of travel through a PPFC without being in contact with the substrate, a SF was designed to ensure uniform cell contact with the substrate from the time they enter the main chromatography channel of the chamber. This feature ensures that a maximum number of the perfused cells interact with the selectin-coated substrate in the main channel, and the ones which settle down have an equal opportunity to interact with the substrate without compromising the channel length during cell settling. Since the RTD studies were conducted by using a small volume of cell solution as a pulse, it is essential to allow as many cells as possible the equal chance of interacting with the substrate.

When determining the shape of the settling feature, COMSOL multiphysics was leveraged to simulate flow within the chamber; this resulted in a desired velocity profile of bulk flow within the feature for several configurations. The circular loop shape for SF was chosen because the COMSOL simulation indicated that the velocity profile within this shape was relatively low compared to other shapes (circular, rectangular, and triangular shapes) without creating too many stagnation zones, where cells can be trapped and form aggregations. Also, in order to prevent PDMS from collapsing, the looping feature was necessary. The maximum aspect ratio (width to height) for the channel was set to be 25.

The benefit of the SF in our PPFC compared to the conventional PPFC is schematically described in Figure 4.1.2.1.

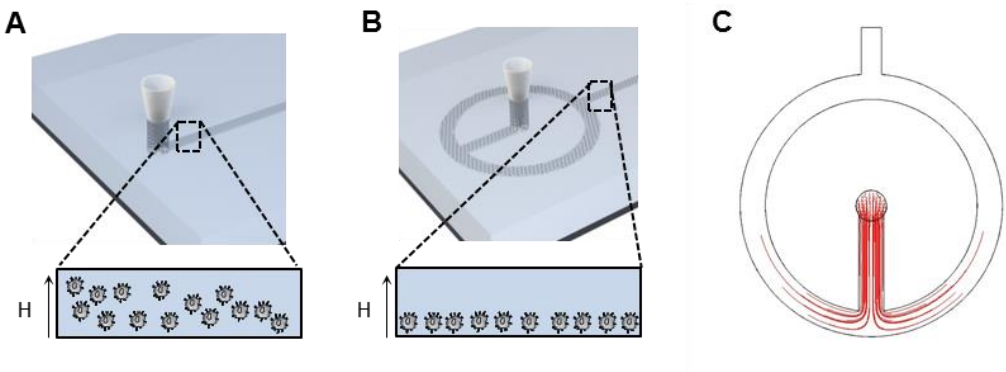

Figure 4.1.2.1. Schematic view of conventional PPFC and cell adhesion chromatography system designed in this work. Different distributions of the cells relative to the bottom of the chamber are schematically described for the conventional (A) and our (B) cell chromatography systems. Inset zoomed views of the entrance to the main channel illustrate the effect of SF on cell settlement. The streamline profile (C) indicates cells' traveling path and the locations where they reach the chamber bottom within the SF.

The SF in our PPFC causes the cells to settle down before entering the main channel, whereas the cells in the conventional PPFC are randomly distributed vertically relative to the chamber bottom at the beginning of the channel as it can be seen in A and B of Figure 4.1.2.1, respectively. The ends of the streamline generated by COMSOL indicate the locations where the cells reach the chamber bottom within the SF (Figure 4.1.2.1.C). The overall schematic view of our PPFC with the SF incorporated at the upstream of the main channel is illustrated in Figure 4.1.2.2.

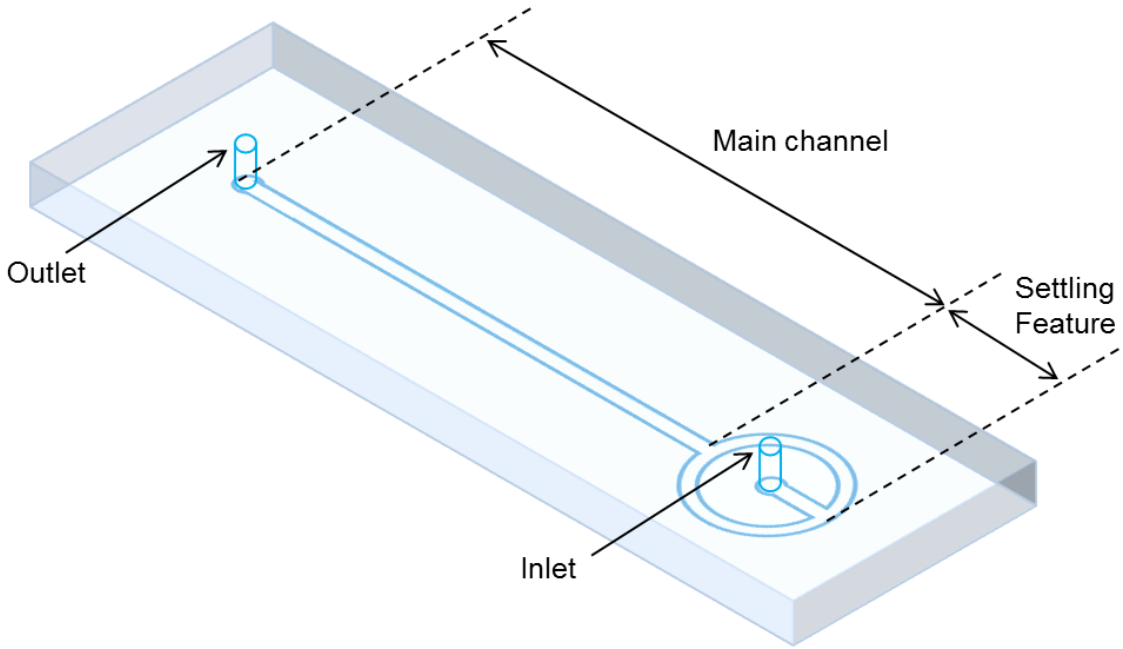

Figure 4.1.2.2. PDMS chamber schematic. A PDMS chamber is composed of an inlet, a settling feature, a main channel, and an outlet.

To determine the equivalent chamber length that the SF effectively provides (albeit without any functionalized adhesive substrate in subsequent work, so ineffectual in its impact in the observed average cell rolling behavior), we performed calculations for three different shear stresses (0.5, 1.0, and 1.5 dyn/cm^2) with three different vertical starting locations for the cells to start traveling (95, 50, and 5 µm from the chamber bottom). Several assumptions were made; 1) cell settling depends only on gravity, thus settling velocity and time are fixed, 2) 0.1% BSA in DPBS (approximated to have the same density as water) is the medium in which the cells settle and travel, 3) the highest and the lowest vertical positions of the cells are 95 and 5 µm, respectively, and 4) bifurcation effects in SF are neglected. In order to find the residence time of the cells within SF, we need to calculate the required times for the cells to settle down and travel along the channel to reach the end of SF. The summation of these two amounts of time is the SF residence time. For

the settling, the velocity of the settling is calculated by utilizing Stokes' law, which describes bulk flow settling solely based on gravity; the equation can be seen in the following (Equation 1).

$$v_{set} = \frac{2}{9} \times \frac{\rho_{cell} - \rho_w}{\mu_w} \times r_{cell}^2 \times g \quad (1)$$

where v_{set} is cell settling velocity, ρ_{cell} is cell mass density, ρ_w is the mass density of water, μ_w is dynamic viscosity of water, r_{cell} is cell radius, g is acceleration due to gravity. The variables are universal throughout this section. Once the settling velocity is determined, the time required for the cells to settle down can be simply calculated by dividing the starting vertical position of the cells within the channel by the settling velocity.

Next, we need to know how long it takes for the cells to travel the remaining distance in SF after they have settled down. However, the distance that the cells travel while settling is not known. In order to calculate this distance, several equations (Equation 2, 3, and 4) are required.

$$y = \frac{h}{2} - v_{set} \times t \quad (2)$$

$$v_x = \frac{\tau_w \times h}{4 \times \mu_w} - \frac{\tau_w}{h * \mu_w} \times y^2 = \frac{\tau_w}{\mu_w} \times v_{set} \times t - \frac{\tau_w}{h * \mu_w} \times v_{set}^2 \times t^2 \quad (3)$$

$$x = \int_0^{t_{set}} v_x \times dt \quad (4)$$

where h is the chamber height, τ_w is shear stress, and t_{set} is settling time. Equation 2 and 3 describe vertical position of the cells and the velocity profile within the chamber, respectively.

Both of these equations are expressed as functions of time to integrate with respect to time as seen in Equation 6. The resultant equation for the integration is Equation 7.

$$x = \frac{\tau_w \times h^2}{6 \times v_{set} \times \mu_w} \tag{7}$$

The distance (x) that the cells travel along the channel while settling down can be obtained by plugging in an h value. However, there are two different shear regions for section 1 and 2 in SF as seen in Figure 4.1.2.3.

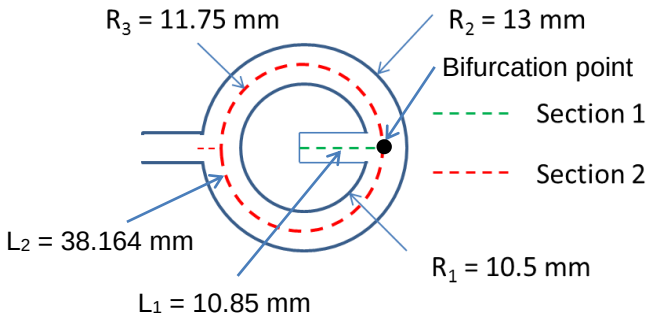

Figure 4.1.2.3. Dimensions of SF with two sections considered for calculating residence time of the cells in SF. Two paths (green and red) for the traveling cells within SF were shown to calculate their residence time in SF. R and L indicate radius and length, respectively.

Therefore, whether or not the cells completely settle down within section 1 has to be determined by using Equation 7 and solving it for h with x being the length of the section 1 (L_1). Also, the shear stress for section 1 has to be used. For the shear stresses considered in this paper, the cells do not reach the bottom of the chamber in the section 1. Therefore, the cells continue settling down in the section 2. In order to find out how far they travel while continuing settling in the section 2 (d_{set2}), Equation 7 is again used to calculate x with h being the remaining height after settling for

a certain amount of height in the section 1 and τ_w being the shear stress in the section 2. With this found, the remaining distance in the section 2 for the cells to travel can be determined by subtracting d_{set2} from the length of the section 2 (L_2). Finally, the time required for the cells to travel the remaining distance in section 2 can be calculated by dividing the distance by the velocity of the cells at the bottom of the chamber, which can be obtained by using Equation 3. Consequently, the residence time is obtained. With the residence time known, the estimation for how far the cells travel in the main channel for the amount of the residence time can be calculated similarly. Equation 7 determines how far the cells travel while settling in the main channel (d_{set_main}). Then, multiplying the velocity of the cells at the bottom of the chamber by the rest of time (residence time – settling time) results in the distance traveled by the cells after settlement (d_{trv_main}). Thus, the cells travel a certain distance ($d_{set\_main} + d_{trv\_main}$) in the main channel given the residence time in SF. Table 4 shows calculated distances for three different shear stresses and staring locations of the cells as well as the corresponding residence times.

Shear stress (dyn/cm2) / Vertical position relative to chamber bottom	0.5	1.0	1.5
95 µm	123 (387)	139 (187)	151 (116)
50 µm	111 (408)	111 (199)	116 (135)
5 µm	111 (416)	111 (208)	111 (138)

Table 4. Cell traveling distances within the main channel for the equivalent SF residence time at different shear stresses and initial vertical locations. The unit for the distances is in mm. Corresponding residence time in second for each case is indicated in parenthesis.

To find out the maximum limit of the shear stress that can be applied to the main channel while achieving complete cell settlement in SF, a simple MATLAB script was written. The calculations involved are explained in the following and the assumptions made are identical to those for the calculation of equivalent traveling distance in the main channel for the residence time the cells spend in SF. The initial position of the cell was set to be 95 µm. By solving Equation 7 for h, how far the cell settles down in the section 1 of SF is determined as seen in Equation 9. Equation 8 expresses the shear stresses in the section 1 and 2 of SF in terms of the one in the main channel.

$$\tau_{SF1} = \frac{1}{1.25}\tau_{main} \;\; \& \;\; \tau_{SF2} = \frac{1}{2}\tau_{SF1} = \frac{1}{2.5}\tau_{main} \tag{8}$$

$$h_{SF1\_set} = \sqrt{\frac{6 \times L_{SF1} \times v_{set} \times \mu_w}{\tau_{SF1}}} = \sqrt{\frac{1.25 \times 6 \times L_{SF1} \times v_{set} \times \mu_w}{\tau_{main}}} \tag{9}$$

where τ_{main}, τ_{SF1}, and τ_{SF2} are wall shear stresses of the main channel, the section 1 and 2 of SF, respectively, h_{SF1_set} is the settling height in the section 1 of SF, L_{SF1} is the section 1 length, v_{set} is the settling velocity, and μ_w is the dynamic viscosity of water. Then, Equation 7 is employed again to calculate how far the cells travel along the channel in SF while settling, which can be seen in Equation 10.

$$x_{trv\_SF2} = \frac{\tau_{SF2} \times (90 - h_{SF1\_set})}{6 \times v_{set} \times \mu_w} = \frac{\tau_{main} \times (90 - h_{SF1\_set})}{2.5 \times 6 \times v_{set} \times \mu_w} \tag{10}$$

where x_{trv_SF2} is the distance traveled by the cell in the section 2 of SF. The term, $(90 - h_{SF1\_set})$, indicates the remaining height that the cell needs to settle down in section 2 before leaving SF. Note that shear stress in x_{trv_SF2} is expressed in terms of τ_{main} to find out its value that results in x_{trv_SF2} to be close to, but not exceeding the length of the section 2 in SF. It its current configuration, this SF is sufficient to result in uniform cell settling up to a shear stress of 5.45 dyn/cm^2.

To find the minimum cell radius that will completely settle within the SF at 1.5 dyn/cm^2, Equation 10 was used to obtain v_{set} with x_{trv_SF2} being the total length of section 2 of SF. With v_{set} value calculated, Equation 1 was used to determine the minimum cell radius by plugging in the values for other parameters, which were stated in Section 3.2. From the calculation, the minimum cell radius that will settle completely within the SF at 1.5 dyn/cm^2 and at the cell density of 1.032 $\times$ 10^3 kg/m^3 is 7.3 µm.

In order to find out the lower bound of cell density to achieve complete cell settling before the main channel, Equation 10 was used to calculate v_{set} that allows the cells to settle down while traveling the entire length of the region 2 of SF with wall shear stress of the main channel to be the maximum shear stress used in this paper, which is 1.5 dyn/cm^2. Then, Equation 1 was used to calculate the mass density of cells with the calculated v_{set} and the values of other parameters (introduced in Section 3.2) plugged in. The lower bound cell density that was determined from these calculations was 1.025 x 10^3 kg/m^3.

Studying adhesive behaviors of the cells over the long main channel in our PPFC requires that the wall shear stress profile to be uniform throughout the channel. In order to find out the shear stress profile in our PPFC, COMSOL was used to simulate the flow, and the results can be seen in Figure 4.1.2.4.

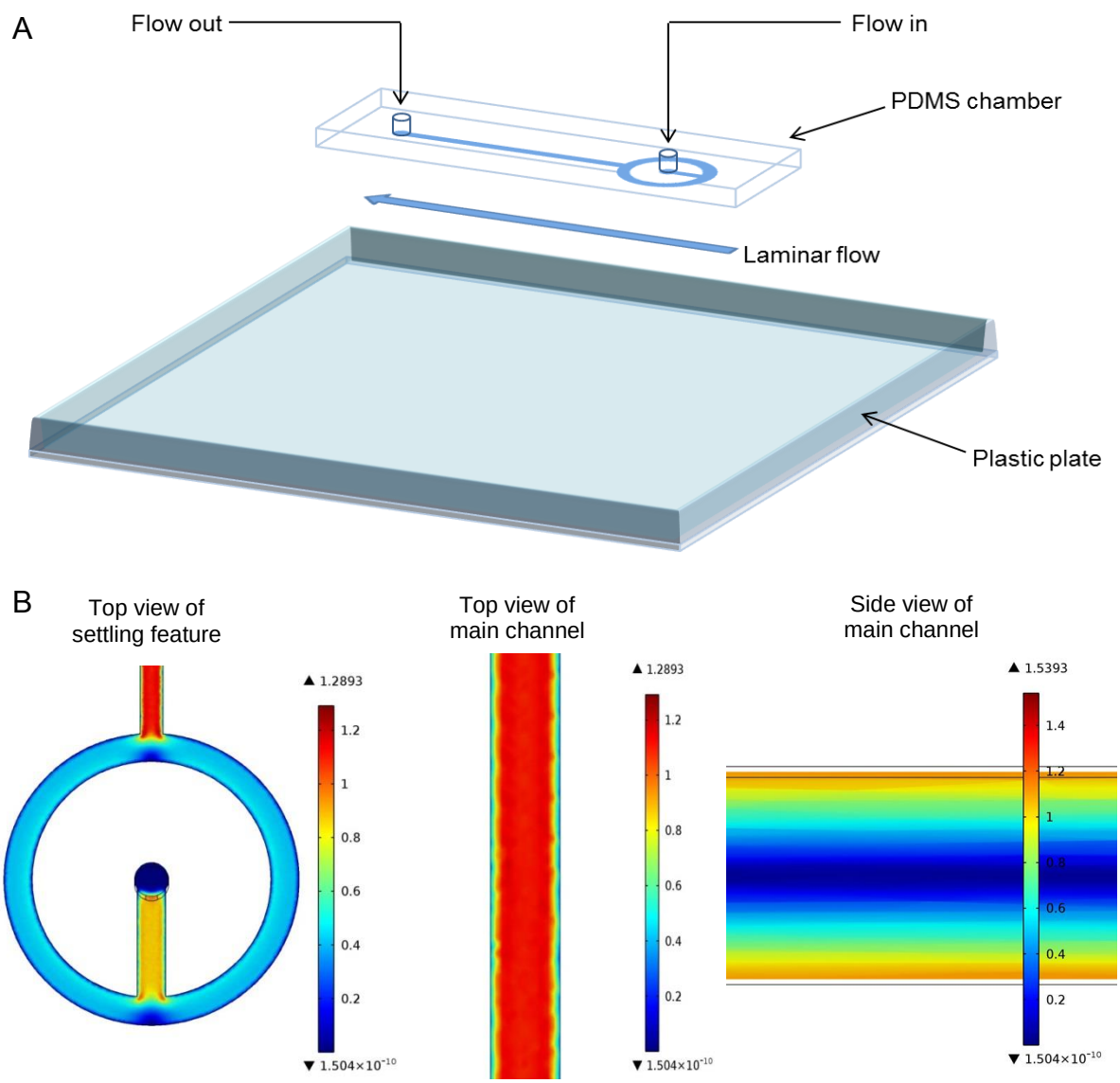

Figure 4.1.2.4. Schematic view of a parallel plate flow chamber and shear profile. All the wall shear stresses used in this paper created laminar flow throughout the chamber (A). Shear profile within the chamber was generated by using COMSOL Multiphysics with a normal inflow velocity of 5.1873×10^{-5} m/sec to the inlet of the chamber, which is required to generate a wall shear stress of 1 dyn/cm^2 for 100 µm height chamber (B).

From the shear profile generated by COMSOL, it was demonstrated that our PPFC was able to generate uniform shear stress profile throughout the channel. Also, the shear profile within the SF revealed that the magnitude of shear stress within the SF was about two-fold less than the one within the main channel. This low shear contributed to the accelerated cell settling within the SF than would be achieved within an equivalent length of the main channel.

4.1.3 Coherence in Chamber Fabrication

To find out if the chamber was made as designed, theoretical and measured velocity of cells at three different wall shear stresses were compared as seen in Figure 4.1.3.

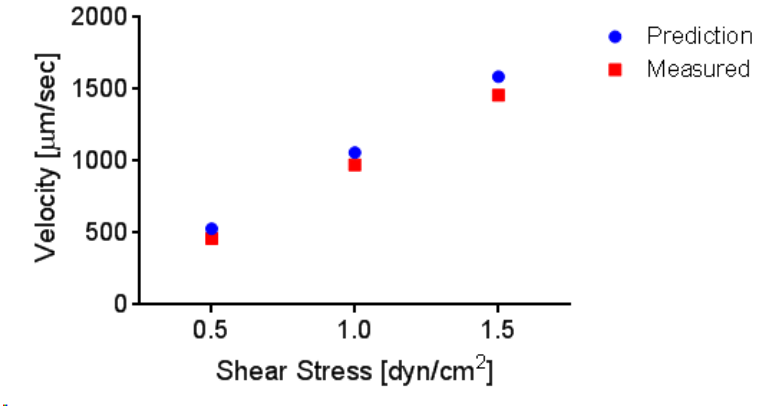

Figure 4.1.3 Predicted versus measured free cell velocity in shear flow. Data for the measured velocity represent means ± SEM.

Cells in the main channel are in close proximity to the substrate, by design, as the result of the SF. Therefore, the theoretical velocity was chosen as the bulk flow velocity at the bottom of the chamber. According to Goldman, hydrodynamic wall effects make the convection velocity at the wall slower than free stream velocity [64]. Therefore, the equation to calculate the theoretical

velocities of the cells at the bottom of the chamber was adopted from Goldman's study, which can be seen in Equation 11.

$$v_x = y\gamma_w \left(1 - \frac{5}{16}\left(\frac{r}{y}\right)^3\right) \tag{11}$$

Y is the vertical position of the cell from the chamber bottom, γ_w is the shear rate, and r is the radius of the cells. All three shear stresses used in this paper were considered to calculate bulk flow velocity at the bottom of the chamber with the previously reported LS174T cell radius of 14 µm [65]. Cells were perfused through the chamber with three different shear stresses and imaged at multiple positions along the channel. Their velocities were then analyzed with CELL TRAKCER and found to be in close agreement with the predicted velocities (Figure 4.1.3).

4.1.4 Vertical Locations of Cells in Chamber

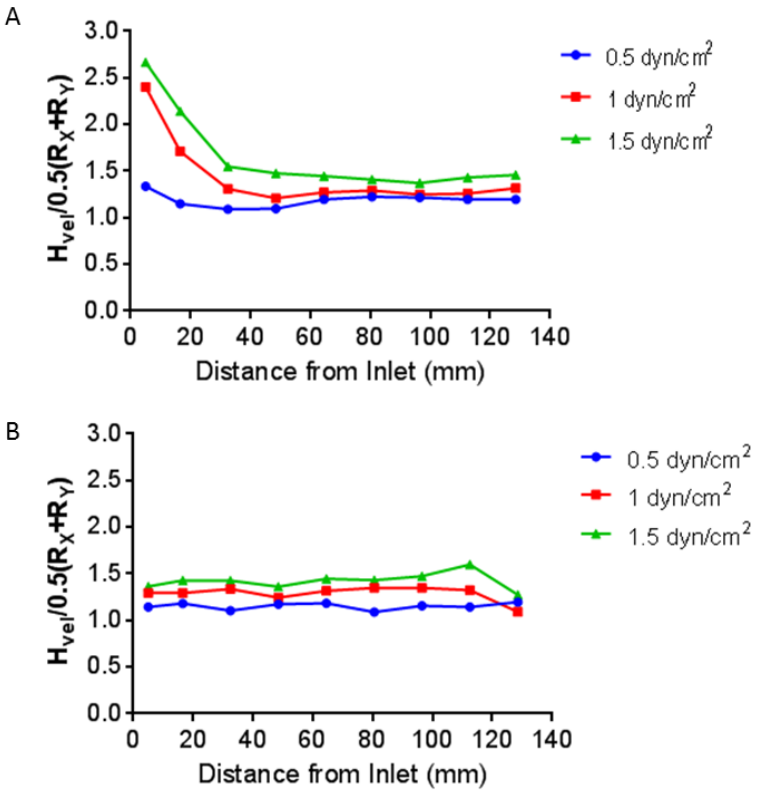

Figure 4.1.4.1 $H_{vel}/0.5(R_x+R_y)$ at various shear stresses for chambers with and without SF. A perfusion experiment was executed by using three different shear stresses and perfusing cells through a chamber with no SF and the inlet with a SF to determine the mean cell distance from the chamber bottom. A metric, ($H_{vel}/0.5(R_x+R_y)$), was employed to estimate cells' vertical position at multiple locations in the chamber. The results indicated that the cells needed about 2, 5, and 10 cm to completely settle to the bottom of the chamber for the shear stress of 0.5, 1.0, and 1.5 dyn/cm^2, respectively, in the chamber without SF (A). With SF, the cells were traveling close to the bottom of the chamber as soon as they entered the main channel (B). Data indicate mean ± SEM.

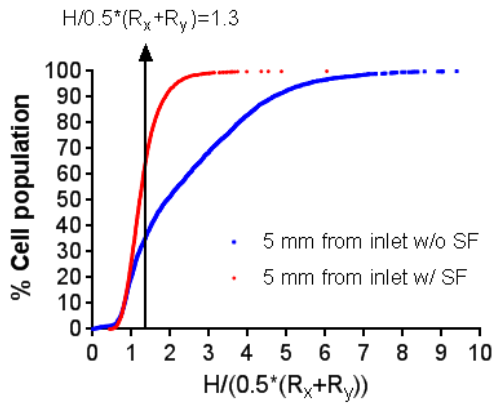

Figure 4.1.4.2 Cumulative distribution function for $H_{vel}/0.5(R_x+R_y)$. Cells were perfused from an inlet and an outlet and imaged at 5 mm after SF and 5 mm from the outlet to determine percent cell population located at a certain vertical position relative to the bottom of the chamber.

To find out how far the cells have to travel along the channel to be in close proximity to the substrate depending on three different wall shear stresses, a perfusion experiment was performed with a blank chamber by injecting cells from the outlet. Videos for imaging freely traveling cells at 9 different locations were generated and analyzed with CELL TRACKER. Data exported from CELL TRACKER contained vertical positions of the cells based on their velocities (H_{vel}) and their radius in x and y directions (R_x and R_y). CELL TRACKER calculates the vertical position of the cells relative to the bottom of the chamber based on the measured velocities of the cells. Solving Equation 3's velocity profile component for y and plugging in the values for the measured velocity, shear stress, chamber height, and dynamic viscosity of water returns the y position of the cells from the mid-plane (at y=0 in the coordinate system). To find out how far the cells are located from the bottom of the chamber, the y position from the mid-plane is subtracted from the half of the chamber height. A metric to determine how close the cells were to the bottom of the chamber was created; it is the fraction of cells' vertical position over effective cell radius

($H_{vel}/0.5(R_x+R_y)$). A value of 1.0 indicates that the cells are at the bottom of the chamber. The results demonstrate that the cells approached the bottom of the chamber at about 2, 5, and 10 cm from where they entered the chamber without the SF for the shear stress of 0.5, 1.0, and 1.5 dyn/cm^2, respectively (4.1.4.1). Therefore, it was shown that SF helps the cells to settle down before entering the main channel, which increases the residence time for the cells. Also, a cumulative distribution function (CDF) for $H_{vel}/0.5(R_x+R_y)$ was generated to find out the percent of total cell population within a certain height from the chamber bottom, which can be seen in Figure 4.1.4.2. At the cut-off line where $H_{vel}/0.5(R_x+R_y)$ value is 1.3, and the cells appears to be at the chamber bottom according to Figure 4.1.4.1, approximately 65% and 35% of the cells is populated for the chamber with and without the SF, respectively. This result shows that the chamber with the SF can at least double the cell population at the bottom of the chamber, compared to the conventional chamber.

4.2 Uniform Chamber Functionalization

In order to uniformly functionalize the main channel of our PPFC with selectins, we developed a protocol as described in chapter 3 (Materials and Methods). The schematic view of the steps taken for chamber functionalization can be seen in Figure 4.2.1.

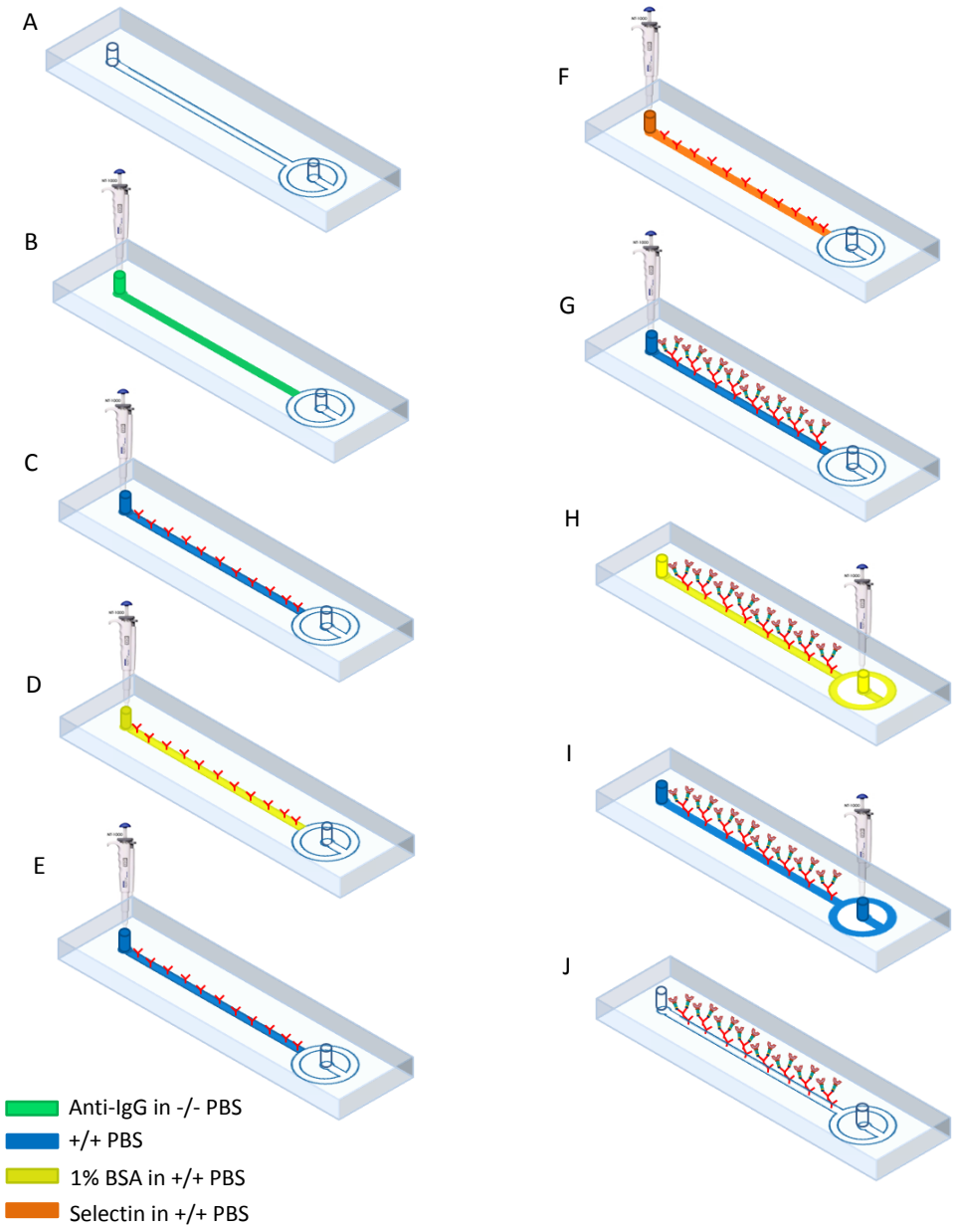

Figure 4.2.1. Schematic view of chamber functionalization. The steps involved in immobilizing selectins to a substrate are the following. A) Prepare a bonded chamber, B) incubate the testing region with Anti-IgG solution at a desired concentration in 4 ˚C overnight, C) wash the testing region with PBS containing Ca^{2+}/Mg^{2+}, D) block the testing region with 1% BSA, E) wash the testing region with PBS containing Ca^{2+}/Mg^{2+}, F) incubate the testing region with selectin solution at a desired concentration, G) wash the testing region with PBS containing Ca^{2+}/Mg^{2+}, H) block

the whole chamber with 1% BSA, and I) wash the whole chamber with PBS containing Ca^{2+}/Mg^{2+}. Finally, J) the chamber functionalized with selectins is ready for an experiment. For steps of A to G, the reagents were infused from the outlet of the chamber to only treat the testing region.

To determine whether the chamber was functionalized with selectin uniformly throughout the channel length, the extent of adhesion along the channel was assessed (Figure 4.2.2).

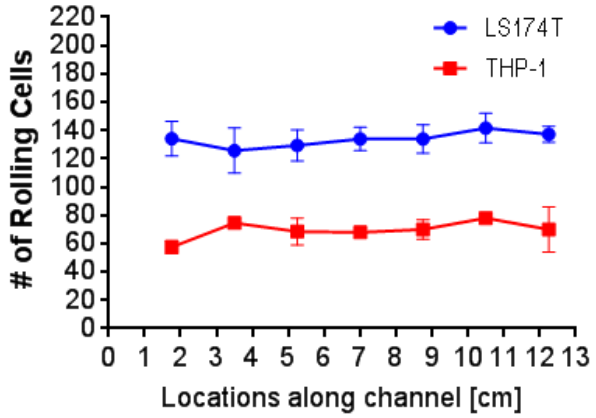

Figure 4.2.2. Extent of adhesion for LS174T and THP-1 cells along a channel length. LS174T (n=6) and THP-1 (n=2) cells (at 5 x 10^5 cells/mL) were perfused over a substrate coated with 25 µg/mL P-selectin with wall shear stress of 1 dyn/cm^2. The extent of adhesion was measured by counting the number of rolling cells at multiple locations along the channel, which were plotted to determine whether or not the substrate was evenly immobilized with P-selectin. Data represent means ± SEM.

Both LS174T and THP-1 cells were perfused over substrates that were coated with 25 µg/mL P-selectin at the wall shear stress of 1 dyn/cm^2. The extent of adhesion at each location was determined by counting the number of cells in the field of view for 1 minute. The results indicate that the substrates were homogenously functionalized with P-selectin as the number of rolling cells

was comparable throughout the channel length. Also, we noticed that THP-1 cells showed less extent of rolling than LS174T. This is because THP-1 cells express high affinity P-selectin ligand, PSGL-1, on their surfaces, which causes THP-1 cells to roll slower than LS174T cells over P-selectin-coated substrates. This resulted in fewer THP-1 cells rolling in the field of view within a one minute timeframe.

4.3 Increase in Residence Time due to Selectins

In order to assess the effects of selectins on residence time of the cells in the chamber, RTD (Residence Time Distribution) experiments were performed. The experimental setup can be seen in Figure 4.3.1.

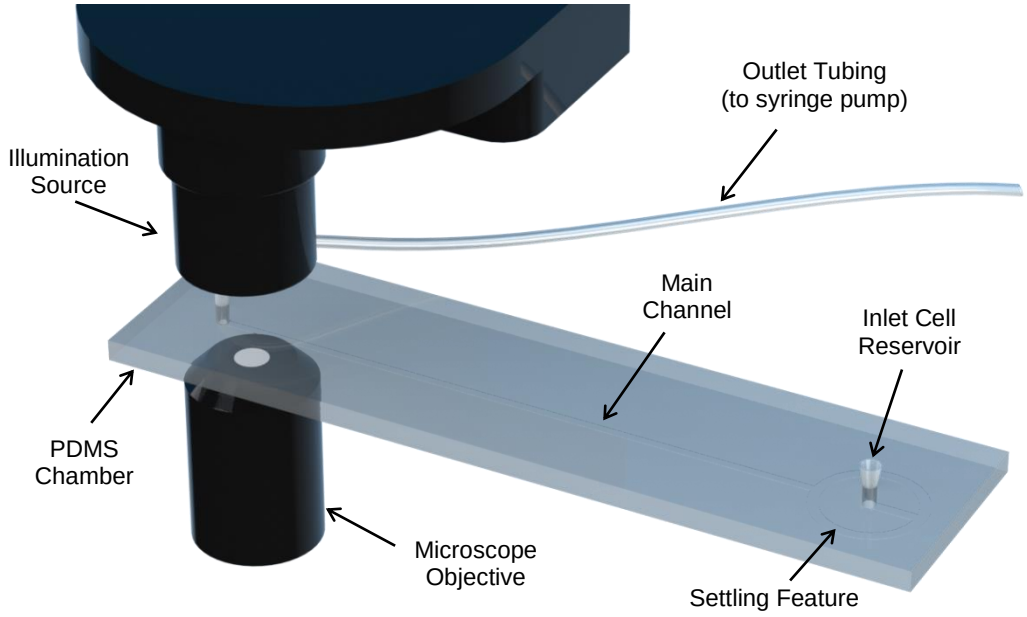

Figure 4.3.1. Schematic view of chamber setup. A pulse cell suspension (at 5×10^5 cells/mL) was perfused through an inlet reservoir of a PDMS chamber to observe adhesive behaviors of the cells over the selectin-coated substrate in the main channel. A field of view was set close to an outlet to

image cell adhesion with a phase contrast microscope. The shear stress in the chamber was determined by a syringe pump connected to the outlet of the chamber.

The main channel (either 1.3 or 14 cm long) of the chamber was functionalized with 25 μg/mL P-selectin. Two different chamber lengths were used for RTD experiments in order to make sure that the whole population of a cell pulse input could be imaged at the elution point (field of view) within a two hour time frame of experimentation. Since two different types of cells studied in this paper express different selectin-ligands with different binding efficiency to selectins, cell populations that exhibit slow rolling velocities (<20 μm/sec) cannot be adequately imaged a with 14 cm-long chamber within two hours. Also, as one of our long-term goals is to fractionate cells based on RTD profiles; a 14 cm-long chamber therefore enhances the resolution and peak separation times of weakly versus strongly interacting cells at the elution point. Using the chambers functionalized with selectins, the cells were perfused over the substrates at three different shear stresses and elution times recorded. Also, the cells were perfused through the blank chambers with three different shear stresses for comparison. The results of the RTD experiments can be seen in Figure 4.3.2.

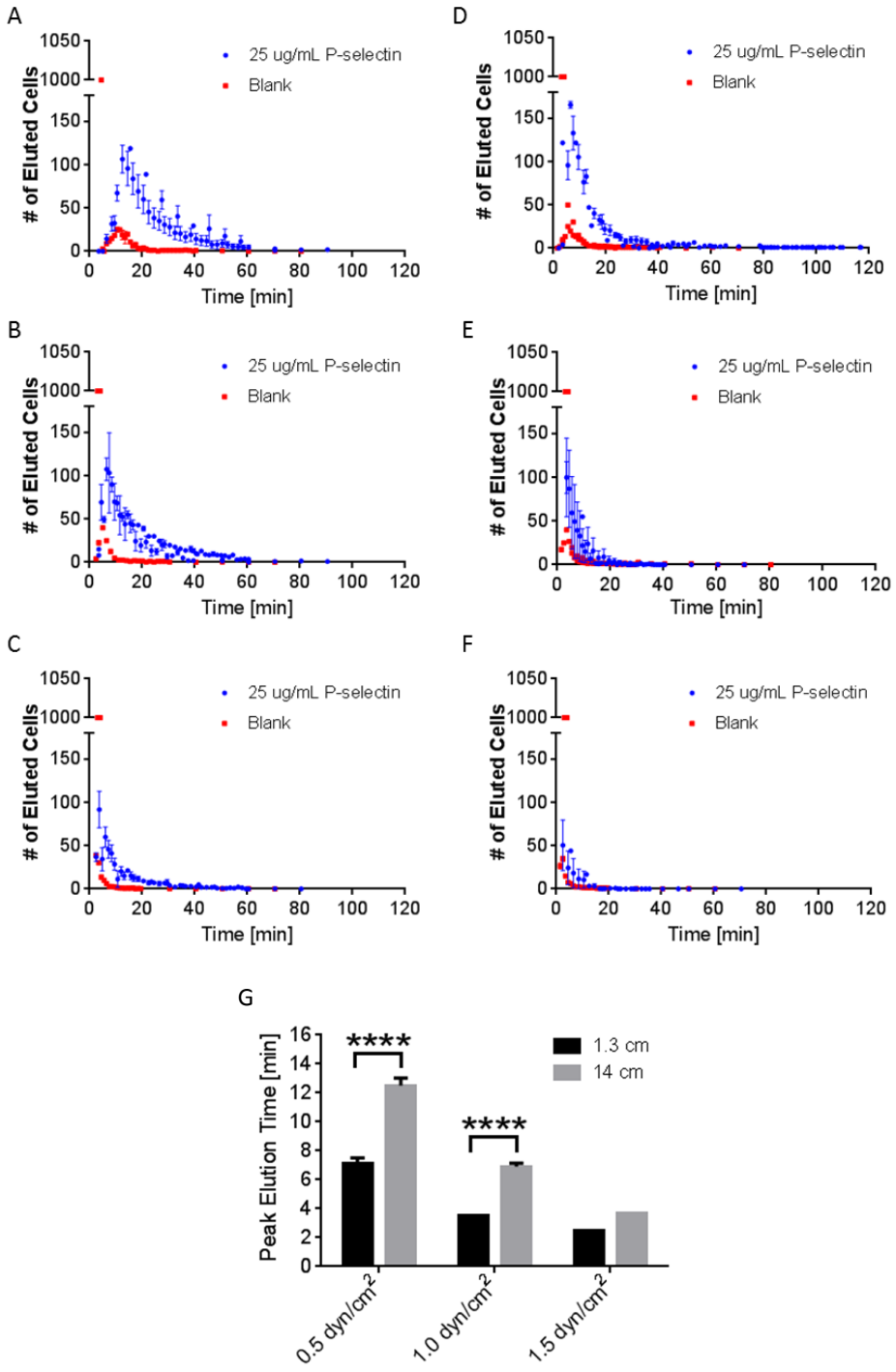

Figure 4.3.2. Residence Time Distribution (RTD) for selectin-coated versus blank chambers. LS174T cells (at 5×10^5 cells/mL) were perfused over 14 (A, B, and C) and 1.3 cm (D, E, and F)-long chambers that were coated with 25 µg/mL P-selectin (Blue) and blocked with 1% BSA (Red)

at 0.5 (A and D), 1.0 (B and E), and 1.5 (C and F) dyn/cm^2. The number of eluted cells for the blank chambers is the average number of cells that passed the field of view for 1 minute. Significant difference in the elution times of LS174T cells over P-selectin chambers (1.3 vs 14 cm) was observed for the wall shear stress of 0.5 and 1.0, but not 1.5 dyn/cm^2 (G).

An arbitrary data point of 1000 was added to Figure 4.3.2 to indicate our inability to manually count all the freely traveling cells that eluted at early time points in unfunctionalized chambers. Since all cells elute within the time frame of experimentation these two curves should have the same integration area. However with our present system of analysis, a more precise quantification is not feasible. Regardless, our data illustrate that the cells perfused through the blank chambers appeared at the field of view earlier than the ones perfused through the chamber functionalized with 25 µg/mL P-selectin. This observation was seen for both lengths of the chambers (1.3 and 14 cm) and three shear stresses (0.5, 1.0, and 1.5 dyn/cm^2). Also, the elution time of the cells increased as the applied shear stress decreased and vice versa. Therefore, it was verified that selectin delayed the elution time of the cells. Furthermore, significant differences in the elution times of LS174T cells perfused through P-selectin chambers with 1.3 and 14 cm lengths were observed at the wall shear stresses of 0.5 and 1.0, but not 1.5 dyn/cm^2.

4.4. Effects of SF on RTD Profiles

To examine the effect of the SF on measured RTDs, RTD experiments were performed by perfusing cells from the inlet versus the outlet of the chamber. RTD profiles generated from the experiments can be seen in Figure 4.4.

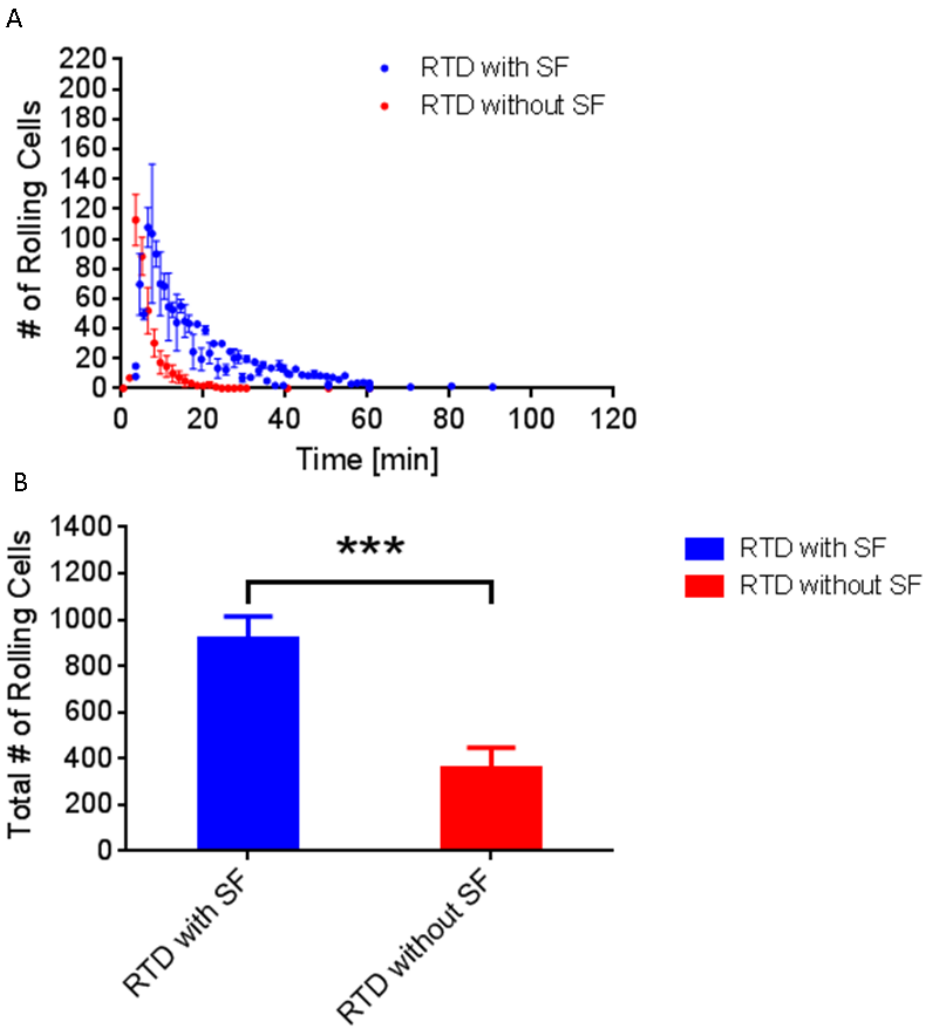

Figure 4.4 RTD profiles from perfusion experiments performed in chambers with and without SF. LS174T cells were perfused through chambers (with and without SF) coated with 25 µg/mL P-selectin at shear stress of 1.0 dyn/cm^2. From the experiments, RTD profiles were generated based on the number of rolling cells counted at the field of view (A). The SF resulted in a significant increase in the number of cells that interacted with the substrate (rolling velocities ~<100 µm/s) in chambers with a SF compared to chambers without a SF (B).

Our data demonstrate that the SF resulted in a significant increase in the number of perfused cells that interacted with the substrate within the chamber compared to when the same experiment was performed in chambers lacking a SF. These results indicate the utility of the SF in increasing the cell contact with the substrate for interrogation of cell adhesion efficiencies in shear flow.

4.5 Influence of Cations on Selectin-Mediated Adhesion

In order to demonstrate that cell adhesion is selectin-dependent, a chelating agent (EDTA) was added to the cell suspension and the perfusion media to deplete cations. Since selectins require cations to bind to their ligands, adding EDTA disrupts selectin-ligand interactions. The impact of EDTA on the extent of cell adhesion to selectin substrates is shown in Figure 4.5.

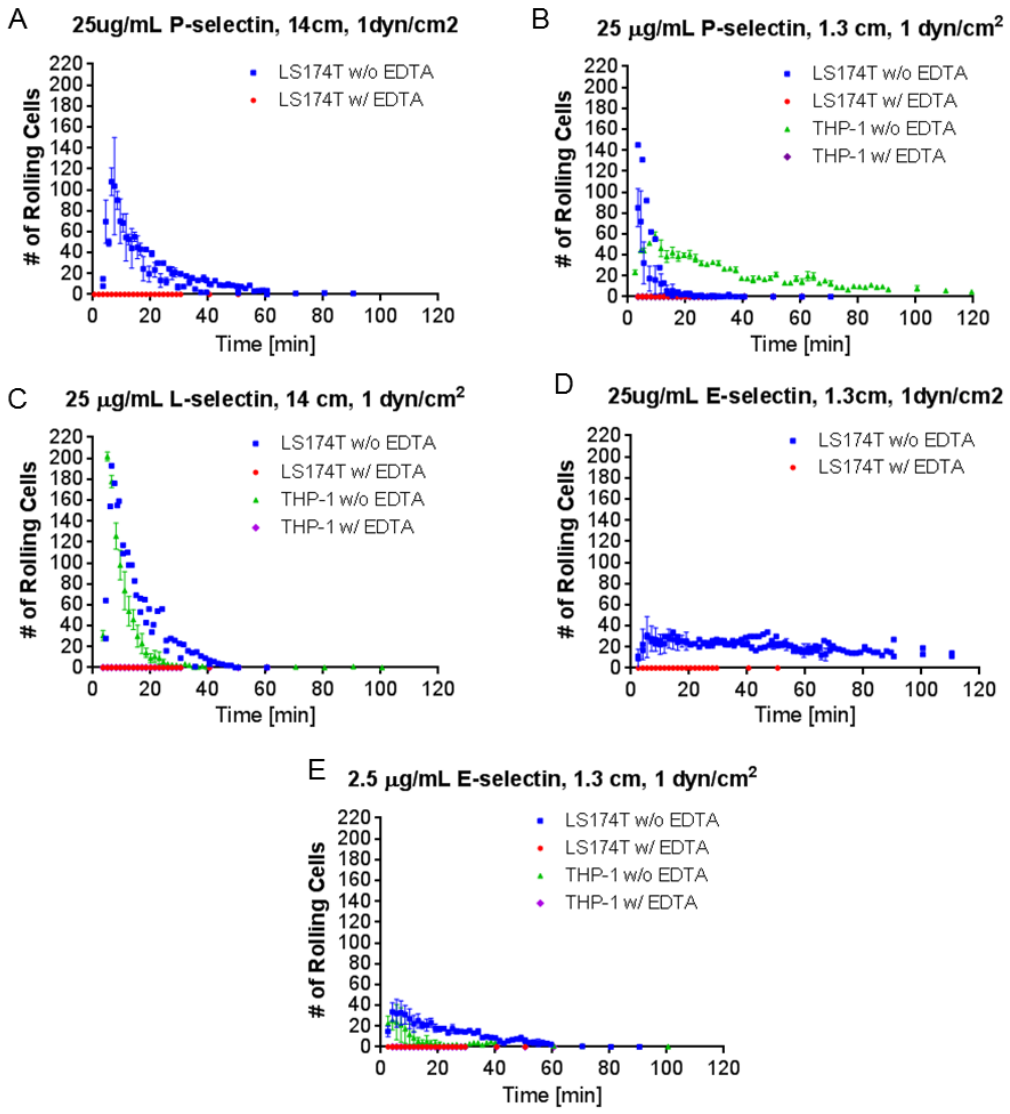

Figure 4.5 Effects of EDTA on cell adhesion. EDTA impaired cell adhesion over a selectin-immobilized substrate, which shows the importance of calcium ions in cell adhesion.

In both cell suspension and perfusion media, the final concentration of 5 mM EDTA was used for RTD experiments. The results indicate that EDTA completely disabled selectin-ligand binding for both types of cells, all tested selectin concentrations, and each class of selectin. These results indicate that cell adhesion in this perfusion system is specifically mediated by selectin.

4.6 Effects of Selectin Concentration on Cell Adhesion

To determine the effects of selectin concentration on the extent of cell adhesion, the number of rolling cells in the field of view at different time points during the course of RTD experiments was recorded and compared accordingly as seen in Figure 4.6. The results indicate a general trend of higher extents of adhesion with higher selectin concentrations.

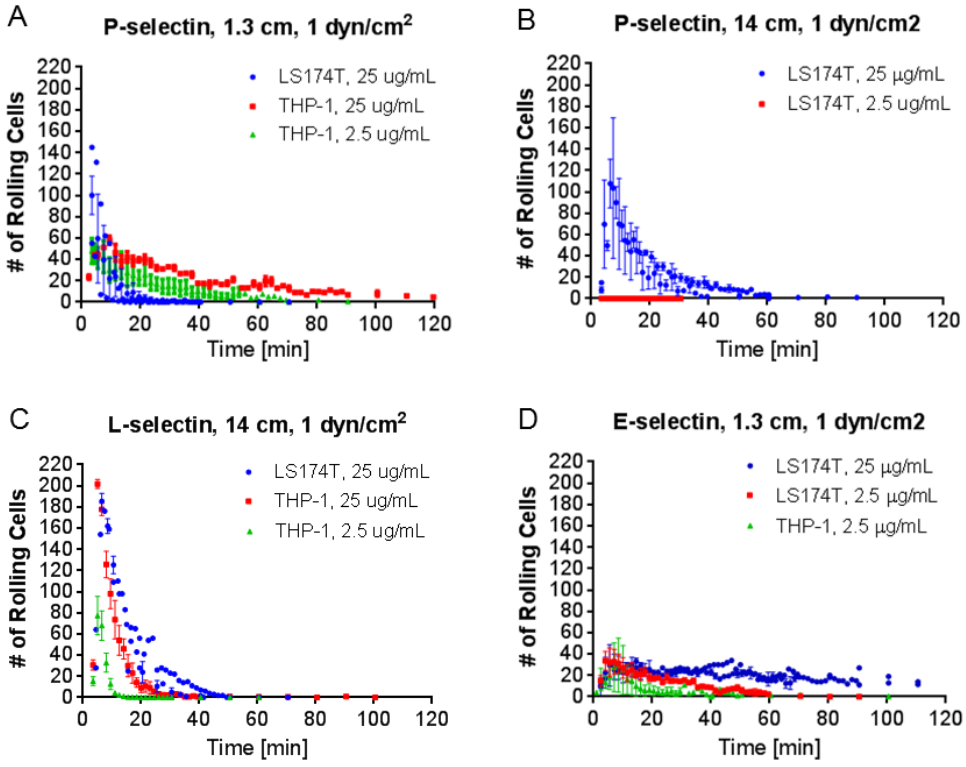

Figure 4.6. The extent of cell adhesion to selectin-coated substrates depends on selectin concentration. Both LS174T and THP-1 cells were perfused (except for B) through the chamber with different lengths and wall shear stress of 1.0 dyn/cm^2. On a P-selectin substrate (1.3 cm-long), THP-1 cells showed higher extent of adhesion than LS174T for both concentrations, and THP-1 cells resided in the chamber longer than LS174T for the concentration of 25 µg/mL (A). On another P-selectin substrate (14 cm-long), only LS174T cells were perfused, and they did not show rolling

for the concentration of 2.5 µg/mL (B). On L-selectin substrate, LS174T cells showed higher extent of adhesion than THP-1 cells for the concentration of 25 µg/mL (C). On E-selectin substrate, LS174T showed higher degree of adhesion than THP-1 cells for the concentration of 2.5 µg/mL (D). Overall, higher concentration of selectin caused higher extent of adhesion. Data present mean ± SEM.

4.7 Effects of Shear Stress on Cell Adhesion

To find out the effects of different shear stresses on the extent of cell adhesion, the number of rolling cells in the field of view at different time points during the course of RTD experiments was recorded and compared accordingly as seen in Figure 4.7.

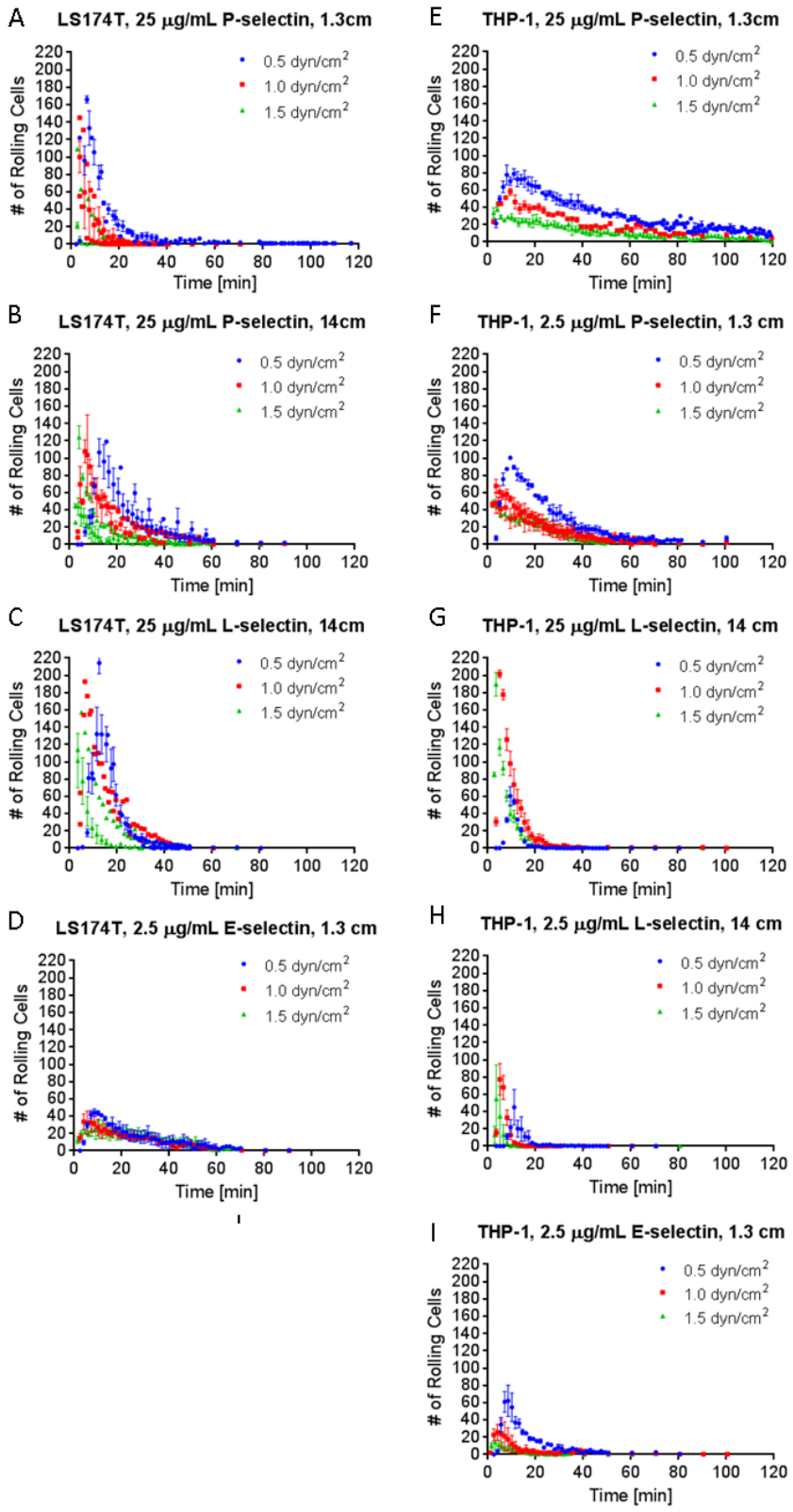
A
LS174T, 25 μg/mL P-selectin, 1.3cm
B
LS174T, 25 μg/mL P-selectin, 14cm
C
LS174T, 25 μg/mL L-selectin, 14cm
D
LS174T, 2.5 μg/mL E-selectin, 1.3 cm
E
THP-1, 25 μg/mL P-selectin, 1.3cm
F
THP-1, 2.5 μg/mL P-selectin, 1.3 cm
G
THP-1, 25 μg/mL L-selectin, 14 cm
H
THP-1, 2.5 μg/mL L-selectin, 14 cm
I
THP-1, 2.5 μg/mL E-selectin, 1.3 cm
# of Rolling Cells
Time [min]
0.5 dyn/cm2
1.0 dyn/cm2
1.5 dyn/cm2

Figure 4.7. Shear-dependent extent of adhesion on selectin-functionalized substrates. LS174T and THP-1 cells were perfused over different lengths of substrates immobilized with three different types of selectins at different concentrations. The results show that increase in shear stress lowers the extent of adhesion (A~F and H~I) except for the one case (G).

The results demonstrate that a higher wall shear stress results in earlier cell elution times regardless of selectin concentration or type. Only THP-1 cells rolling on a L-selectin substrate with a concentration of 25 µg/mL exhibited a different adhesive behavior; a shear stress of 1.0 dyn/cm^2 delayed elution times relative to 0.5 dyn/cm^2. This might be due to flow-enhanced cell adhesion phenomena as described in Section 1.2.3. Also, note that this behavior was not evidenced for 2.5 µg/mL L-selectin as seen in H of Figure 4.7. From this result, it can be postulated that selectin concentration can influence shear-dependent cell adhesion as the cells might need a certain site density of selectin for flow-enhanced cell adhesion to transpire.

4.8. RTD Comparisons between Cell Types

In order to determine whether different cell types exhibit different average interaction behaviors based on RTD profiles, difference in peak elution times were compared (Figure 4.8).

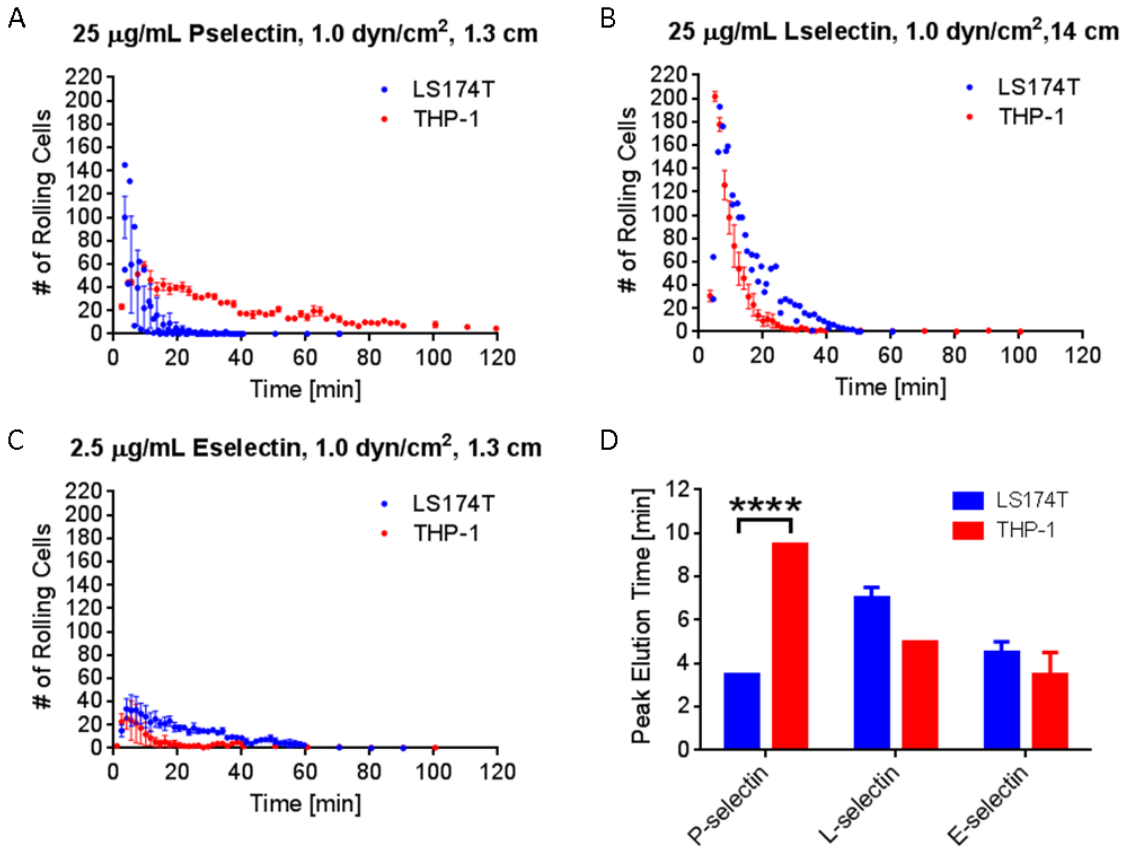

Figure 4.8 RTD profile comparisons between LS174T and THP-1 cells. RTD profiles of two different cell types perfused over three different types of selectins, P (A)-, L (B)-, and E (C)-selectin, at wall shear stress of 1 dyn/cm^2 were generated with statistical analysis on peak time points of RTDs. (D) THP-1 cells demonstrate significantly delayed elution compared to LS174T cells over P-, but not L- or E-, selectin.

LS174T and THP-1 cells perfused over 25 μg/mL P-selectin show significant differences in peak elution times whereas no differences were observed in their elution profiles over L- and E-selectin. On 25 μg/mL P-selectin substrates (1.3 cm-long), THP-1 cells eluted past 60-minute time point, whereas the last LS174T cell was seen around the 35-minute time point. This indicates that on average THP-1 cells have higher avidities for P-selectin than LS174T. On the substrates coated

with 25 µg/mL of L-selectin (14 cm-long), LS174T cells showed slightly earlier but not statistically different elution times than THP-1 cells even though the maximum number of rolling cells was comparable. On 2.5 µg/mL E-selectin substrates (1.3 cm-long), no differences in peak elution times between cell types were observed, though the THP-1 cells took considerably longer to elute from the chamber relative to the LS174T cells.

CHAPTER 5

DISCUSSION

The primary sequences of three selectins were studied in 1989 [19], and the search for their ligands began in parallel. As research progressed, their functional roles were discovered by *in vivo* and *in vitro* cell-binding assays. Leukocyte homing to the site of inflammation and cancer cells metastasizing to a remote location in the vasculature are examples demonstrating the crucial function of selectin-ligand interactions involved in physiological and pathophysiological conditions, respectively. Research has been actively directed towards the description of single molecule biophysics, such as binding rate constant, bond lifetime, and bond reactive compliance, of selectin-ligand interactions in order to identify their force dependencies [5,49,51,53–55], at both the molecular and micro scale. However the macroscale, the length scales over which homing occurs, has been largely overlooked. It remains unclear how persistent selectin-ligand binding is during the cell adhesion process in the circulatory system.

Herein, we introduce a cell chromatography system that was designed to interrogate for the first time the adhesive behavior of cells with selectins at different length scales for extended times. This provides representative insight into the time-averaged behavior of cell-cell interactions occurring in the circulation. One can consider employing our system to study the cancer metastasis in a time-averaged fashion. This is physiologically relevant because in order for blood-borne metastasis to occur, metastatic cells must sustain interactions with the vascular endothelium to eventually extravasate and colonize a distant tissue. The long term goal is to use this system to distinguish the adhesion behavior of healthy versus diseased (malignant) cells, despite even comparable instantaneous binding activities. This platform could be used as a testing device to

validate potential therapeutics for the selective interference with malignant but not healthy cell adhesion in the vasculature. Based on our results, P-selectin is a viable target for interventions aiming to selectively attenuate metastasis since LS174T cells exhibit significantly reduced average affinities (based on mode elution times) for P-selectin in shear flow compared to THP-1 cells. However these results remain to be validated using another cell malignant cell type.

This cell affinity chromatography system was designed to exploit gravity as a means to ensure uniform cell contact with the substrate upon entry into the main channel. We designed a major feature, called the SF, to bring as many cells as possible in the proximity of the substrate within the SF in order to avoid compromising the length of the testing region. This feature is also very important because maximum interaction between cells and the substrate is vital for precisely delineating the adhesive behavior of a population of cells. There are other techniques to induce cell settlement in the application of cell fractionation, such as dielectrophoresis [66] and directed fluid transport [67]. However, these necessitate special equipment and a complex design. The SF incorporated in our system is superior to the aforementioned techniques owing to its simplicity, its independence of other equipment, and its effectiveness, as demonstrated by the results shown in Figure 4.1.4.1 and 4.1.4.2.

The cell chromatography system requires homogeneous distribution of adhesion molecules throughout the channel. This ensures high performance of cell separation without losing a good portion of cells due to areas coated with less density of adhesion molecules. In our system, evenly distributed selectin throughout the channel is also very crucial to correctly extract representative adhesive behaviors of the cells in a lengthy channel. In order to verify the degree of even distribution of selectins in the chamber, we performed cell adhesion assays on the substrate functionalized with 25 µg/mL P-selectin. Seven locations along the channel were imaged to count

the number of rolling cells. The results showed comparable numbers of rolling cells throughout the channel for both types of the cells, LS174T and THP-1. This indicates that selectins were homogeneously immobilized on the substrate, which meets one of the critical requirements of our system.

To study cell adhesion as seen in biological systems, our system needs to be able to create various microenvironmental conditions. In this regard, we examined the adhesive behavior of the cells under different conditions. We varied types and concentrations of selectins on the substrate and studied the corresponding cell adhesion behavior of two different types of cells, LS174T and THP-1. For both LS174T and THP-1 cells, higher concentrations of selectin showed increased adhesion to the substrates with variable extents depending on selectin type. Also, different types of selectin exhibited different characteristic resident time distributions. Our data demonstrate significant differences in LS174T and THP-1 cells interactions with P-selectin based on RTD profiles.

Collectively, we designed a microfluidic cell chromatography system that is equipped with an innovative SF in order to study the time-averaged adhesive behavior of cells over long length scales for extended times. Use of this system in cell adhesion experiments could help broaden our understanding of selectin-ligand cell binding biophysics as well as identify new therapeutic targets for the selective attenuation or promotion of adhesion of specific cell types in the vasculature.

CHAPTER 6

CONCLUSION AND FUTURE WORK

In this work, we developed a platform to study the adhesive behavior of cells mediated between selectins and their cognate ligands. With our cell adhesion chromatography system equipped with the aforementioned functionalities, we can survey different time-averaged adhesive behaviors of different types of cells. In ongoing work, we seek to better characterize the long time and length scale adhesive behavior of a variety of colon carcinoma cell lines to establish an adhesive signature distinct from that of healthy immune cells. Furthermore, future work will include use of this system to fractionate cells based on their chamber residence times within the chamber for in depth molecular and gene expression profiling. The goal will be to identify molecular targets for therapeutic strategies to attenuate metastasis while minimally impacting normal cell homing processes.

APPENDIX A

CELL TRACKER

In order to analyze videos generated from experiments, a custom-built cell-tracking program, called “CELL TRACKER”, was made by using MATLAB (ver. 12.7.0, Mathworks, Natick, MA) by P. Mason McClatchey. User provided parameters for analysis include frames per second (fps), exposure time, resolution, minimum cell diameter, divergence angle, and shear stress, cell’s travel direction, and threshold gain. The algorithm for CELL TRACKER that processes the exported videos and tracks the cells is discussed in the following. CELL TRAKCER uses fps values to determine the total number of frames for the entire length of the videos. It then rotates the frames to correct the orientation based on the cells’ traveling direction at the imaging site. Next, contrast is applied to the frames in accordance with the threshold gain value to detect the edges of the cells. The threshold gain value is tuned before processing the whole video to ensure appropriate detection of the cells and their outlines. Once the suitable threshold gain value is set, the x and y positions of each cell are stored in the first frame. Debris that is smaller than the user-defined minimum cell diameter is excluded, which is useful to prevent small particle ames the cells that are at the next probable positions to which the previously detected cells could have moved are recorded with their positions, shapes, and sizes. When considering the next probable position, the user-provided divergence angle determines how wide a y direction the program should scan for the individual cells’ positions in the next frame. To ensure that the measured average rolling velocities of the cells are representative, CELL TRACKER is programmed not to take into account the data for the cells that have been tracked less than five

frames. In effect, the program will only store data for the cells that have been continuously detected in at least five successive frames or more.

BIBLIOGRAPHY

1. Granger, D. N. & Senchenkova, E. *Inflammation and the Microcirculation*. *Colloq. Ser. Integr. Syst. Physiol. From Mol. to Funct.* **2,** 1–87 (Morgan & Claypool Life Sciences, 2010).

2. Zarbock, A., Kempf, T., Wollert, K. C. & Vestweber, D. Leukocyte integrin activation and deactivation: novel mechanisms of balancing inflammation. *J. Mol. Med. (Berl).* **90,** 353–9 (2012).

3. Sheikh, S., Rainger, G. E., Gale, Z., Rahman, M. & Nash, G. B. Exposure to fluid shear stress modulates the ability of endothelial cells to recruit neutrophils in response to tumor necrosis factor-alpha: a basis for local variations in vascular sensitivity to inflammation. *Blood* **102,** 2828–34 (2003).

4. Malek, A. M. Hemodynamic Shear Stress and Its Role in Atherosclerosis. *JAMA* **282,** 2035 (1999).

5. Yago, T. *et al.* Catch bonds govern adhesion through L-selectin at threshold shear. *J. Cell Biol.* **166,** 913–23 (2004).

6. Thomas, W. E., Trintchina, E., Forero, M., Vogel, V. & Sokurenko, E. V. Bacterial adhesion to target cells enhanced by shear force. *Cell* **109,** 913–23 (2002).

7. Konstantopoulos, K. & Thomas, S. N. Cancer cells in transit: the vascular interactions of tumor cells. *Annu. Rev. Biomed. Eng.* **11,** 177–202 (2009).

8. Läubli, H. & Borsig, L. Selectins promote tumor metastasis. *Semin. Cancer Biol.* **20,** 169–77 (2010).

9. Gahmberg, C. G. *et al.* Leukocyte adhesion--a fundamental process in leukocyte physiology. *Braz. J. Med. Biol. Res.* **32,** 511–7 (1999).

10. McEver, R. P., Beckstead, J. H., Moore, K. L., Marshall-Carlson, L. & Bainton, D. F. GMP-140, a platelet alpha-granule membrane protein, is also synthesized by vascular endothelial cells and is localized in Weibel-Palade bodies. *J. Clin. Invest.* **84,** 92–9 (1989).

11. Setiadi, H. & McEver, R. P. Signal-dependent distribution of cell surface P-selectin in clathrin-coated pits affects leukocyte rolling under flow. *J. Cell Biol.* **163,** 1385–95 (2003).

12. Chen, M. & Geng, J.-G. P-selectin mediates adhesion of leukocytes, platelets, and cancer cells in inflammation, thrombosis, and cancer growth and metastasis. *Arch. Immunol. Ther. Exp. (Warsz).* **54,** 75–84 (2006).

13. Palabrica, T. *et al.* Leukocyte accumulation promoting fibrin deposition is mediated in vivo by P-selectin on adherent platelets. *Nature* **359,** 848–51 (1992).

14. Aigner, S. *et al.* CD24 mediates rolling of breast carcinoma cells on P-selectin. *FASEB J.* **12,** 1241–51 (1998).

15. Cummings, R. D. & Smith, D. F. The selectin family of carbohydrate-binding proteins: structure and importance of carbohydrate ligands for cell adhesion. *Bioessays* **14,** 849–56 (1992).

16. Mannori, G. *et al.* Differential colon cancer cell adhesion to E-, P-, and L-selectin: role of mucin-type glycoproteins. *Cancer Res.* **55,** 4425–31 (1995).

17. Kneuer, C., Ehrhardt, C., Radomski, M. W. & Bakowsky, U. Selectins--potential pharmacological targets? *Drug Discov. Today* **11,** 1034–40 (2006).

18. Burdick, M. M., Bochner, B. S., Collins, B. E., Schnaar, R. L. & Konstantopoulos, K. Glycolipids support E-selectin-specific strong cell tethering under flow. *Biochem. Biophys. Res. Commun.* **284,** 42–9 (2001).

19. Bevilacqua, M. P. & Nelson, R. M. Selectins. *J. Clin. Invest.* **91,** 379–87 (1993).

20. Glycoprotein, A. M. *et al.* Characterization of a Specific Ligand for P-selectin on Myeloid Cells. 12764–12774 (1993).

21. Li, F. *et al.* Post-translational modifications of recombinant P-selectin glycoprotein ligand-1 required for binding to P- and E-selectin. *J. Biol. Chem.* **271,** 3255–64 (1996).

22. Sundd, P., Pospieszalska, M. K., Cheung, L. S.-L., Konstantopoulos, K. & Ley, K. Biomechanics of leukocyte rolling. *Biorheology* **48,** 1–35 (2011).

23. McEver, R. P. & Cummings, R. D. Perspectives series: cell adhesion in vascular biology. Role of PSGL-1 binding to selectins in leukocyte recruitment. *J. Clin. Invest.* **100,** 485–91 (1997).

24. Cummings, R. D. Structure and function of the selectin ligand PSGL-1. *Braz. J. Med. Biol. Res.* **32,** 519–28 (1999).

25. Baumheter, S. *et al.* Binding of L-selectin to the vascular sialomucin CD34. *Science* **262,** 436–8 (1993).

26. Lanza, F., Healy, L. & Sutherland, D. R. Structural and functional features of the CD34 antigen: an update. *J. Biol. Regul. Homeost. Agents* **15,** 1–13 (2001).

27. Katayama, Y., Hidalgo, A., Chang, J., Peired, A. & Frenette, P. S. CD44 is a physiological E-selectin ligand on neutrophils. *J. Exp. Med.* **201,** 1183–9 (2005).

28. Dimitroff, C. J., Lee, J. Y., Rafii, S., Fuhlbrigge, R. C. & Sackstein, R. CD44 is a major E-selectin ligand on human hematopoietic progenitor cells. *J. Cell Biol.* **153,** 1277–86 (2001).

29. Hakomori, S. Aberrant glycosylation in cancer cell membranes as focused on glycolipids: overview and perspectives. *Cancer Res.* **45,** 2405–14 (1985).

30. Hanley, W. D., Burdick, M. M., Konstantopoulos, K. & Sackstein, R. CD44 on LS174T colon carcinoma cells possesses E-selectin ligand activity. *Cancer Res.* **65,** 5812–7 (2005).

31. Napier, S. L., Healy, Z. R., Schnaar, R. L. & Konstantopoulos, K. Selectin ligand expression regulates the initial vascular interactions of colon carcinoma cells: the roles of CD44v and alternative sialofucosylated selectin ligands. *J. Biol. Chem.* **282,** 3433–41 (2007).

32. Thomas, S. N., Zhu, F., Schnaar, R. L., Alves, C. S. & Konstantopoulos, K. Carcinoembryonic antigen and CD44 variant isoforms cooperate to mediate colon carcinoma cell adhesion to E- and L-selectin in shear flow. *J. Biol. Chem.* **283,** 15647–55 (2008).

33. Hanley, W. D. *et al.* Variant isoforms of CD44 are P- and L-selectin ligands on colon carcinoma cells. *FASEB J.* **20,** 337–9 (2006).

34. Nielsen, J. S. & McNagny, K. M. Novel functions of the CD34 family. *J. Cell Sci.* **121,** 4145–4145 (2008).

35. Doyonnas, R. *et al.* Anuria, omphalocele, and perinatal lethality in mice lacking the CD34-related protein podocalyxin. *J. Exp. Med.* **194,** 13–27 (2001).

36. Thomas, S. N., Schnaar, R. L. & Konstantopoulos, K. Podocalyxin-like protein is an E-/L-selectin ligand on colon carcinoma cells: comparative biochemical properties of selectin ligands in host and tumor cells. *Am. J. Physiol. Cell Physiol.* **296,** C505–13 (2009).

37. Larsson, a *et al.* Overexpression of podocalyxin-like protein is an independent factor of poor prognosis in colorectal cancer. *Br. J. Cancer* **105,** 666–72 (2011).

38. Somasiri, A. *et al.* Overexpression of the Anti-Adhesin Podocalyxin Is an Independent Predictor of Breast Cancer Progression Advances in Brief Overexpression of the Anti-Adhesin Podocalyxin Is an Independent Predictor of Breast Cancer Progression. 5068–5073 (2004).

39. Dallas, M. R. *et al.* Sialofucosylated podocalyxin is a functional E- and L-selectin ligand expressed by metastatic pancreatic cancer cells. *Am. J. Physiol. Cell Physiol.* **303,** C616–24 (2012).

40. Osawa, K., Takami, N., Shiozawa, K., Hashiramoto, a & Shiozawa, S. Death receptor 3 (DR3) gene duplication in a chromosome region 1p36.3: gene duplication is more prevalent in rheumatoid arthritis. *Genes Immun.* **5,** 439–43 (2004).

41. Gout, S., Morin, C., Houle, F. & Huot, J. Death receptor-3, a new E-Selectin counter-receptor that confers migration and survival advantages to colon carcinoma cells by triggering p38 and ERK MAPK activation. *Cancer Res.* **66,** 9117–24 (2006).

42. Tan, K. B. *et al.* Characterization of a novel TNF-like ligand and recently described TNF ligand and TNF receptor superfamily genes and their constitutive and inducible expression in hematopoietic and non-hematopoietic cells. *Gene* **204,** 35–46 (1997).

43. Marsters, S. a *et al.* Apo-3, a new member of the tumor necrosis factor receptor family, contains a death domain and activates apoptosis and NF-kappa B. *Curr. Biol.* **6,** 1669–76 (1996).

44. Ahnen, D. J., Nakane, P. K. & Brown, W. R. Ultrastructural localization of carcinoembryonic antigen in normal intestine and colon cancer. Abnormal distribution of cea on the surfaces of colon cancer cells. *Cancer* **49,** 2077–2090 (1982).

45. Gold, P. SPECIFIC CARCINOEMBRYONIC ANTIGENS OF THE HUMAN DIGESTIVE SYSTEM. *J. Exp. Med.* **122,** 467–481 (1965).

46. Hostetter, R. B. *et al.* Carcinoembryonic antigen as a selective enhancer of colorectal cancer metastasis. *J. Natl. Cancer Inst.* **82,** 380–5 (1990).

47. Finger, E. B. *et al.* Adhesion through L-selectin requires a threshold hydrodynamic shear. *Nature* **379,** 266–9 (1996).

48. Chang, K. C., Tees, D. F. & Hammer, D. a. The state diagram for cell adhesion under flow: leukocyte rolling and firm adhesion. *Proc. Natl. Acad. Sci. U. S. A.* **97,** 11262–7 (2000).

49. Chen, S. & Springer, T. a. Selectin receptor-ligand bonds: Formation limited by shear rate and dissociation governed by the Bell model. *Proc. Natl. Acad. Sci. U. S. A.* **98,** 950–5 (2001).

50. Lü, S., Ye, Z., Zhu, C. & Long, M. Quantifying the effects of contact duration, loading rate, and approach velocity on P-selectin–PSGL-1 interactions using AFM. *Polymer (Guildf).* **47,** 2539–2547 (2006).

51. Wayman, A. M., Chen, W., McEver, R. P. & Zhu, C. Triphasic force dependence of E-selectin/ligand dissociation governs cell rolling under flow. *Biophys. J.* **99,** 1166–74 (2010).

52. Thomas, W. E., Vogel, V. & Sokurenko, E. Biophysics of catch bonds. *Annu. Rev. Biophys.* **37,** 399–416 (2008).

53. Zhu, C., Yago, T., Lou, J., Zarnitsyna, V. I. & McEver, R. P. Mechanisms for flow-enhanced cell adhesion. *Ann. Biomed. Eng.* **36,** 604–21 (2008).

54. Marshall, B. T. *et al.* Direct observation of catch bonds involving cell-adhesion molecules. *Nature* **423,** 190–3 (2003).

55. Li, Q., Fang, Y., Ding, X. & Wu, J. Force-dependent bond dissociation govern rolling of HL-60 cells through E-selectin. *Exp. Cell Res.* **318,** 1649–58 (2012).

56. Hinterdorfer, P. & Dufrêne, Y. F. Detection and localization of single molecular recognition events using atomic force microscopy. **3,** (2006).

57. Evans, E., Berk, D. & Leung, a. Detachment of agglutinin-bonded red blood cells. I. Forces to rupture molecular-point attachments. *Biophys. J.* **59,** 838–48 (1991).

58. Evans, E., Ritchie, K. & Merkel, R. Sensitive force technique to probe molecular adhesion and structural linkages at biological interfaces. *Biophys. J.* **68,** 2580–7 (1995).

59. Evans, E., Leung, a, Hammer, D. & Simon, S. Chemically distinct transition states govern rapid dissociation of single L-selectin bonds under force. *Proc. Natl. Acad. Sci. U. S. A.* **98,** 3784–9 (2001).

60. Giavazzi, R., Foppolo, M., Dossi, R. & Remuzzi, a. Rolling and adhesion of human tumor cells on vascular endothelium under physiological flow conditions. *J. Clin. Invest.* **92,** 3038–44 (1993).

61. Rupprecht, P. *et al.* A tapered channel microfluidic device for comprehensive cell adhesion analysis, using measurements of detachment kinetics and shear stress-dependent motion. *Biomicrofluidics* **6,** 14107–1410712 (2012).

62. Martines, E., McGhee, K., Wilkinson, C. & Curtis, A. A parallel-plate flow chamber to study initial cell adhesion on a nanofeatured surface. *IEEE Trans. Nanobioscience* **3,** 90–5 (2004).

63. Herman, C. T., Potts, G. K., Michael, M. C., Tolan, N. V & Bailey, R. C. Probing dynamic cell-substrate interactions using photochemically generated surface-immobilized gradients: application to selectin-mediated leukocyte rolling. *Integr. Biol. (Camb).* **3,** 779–91 (2011).

64. Goldmant, A. J., Cox, R. G. & Brenner, H. Slow viscous motion of a sphere parallel to a plane wall-II Couette flow. **22,** 653–660 (1967).

65. Xue, L. Y., Butler, N. J., Makrigiorgos, G. M., Adelstein, S. J. & Kassis, A. I. Bystander effect produced by radiolabeled tumor cells in vivo. *Proc. Natl. Acad. Sci. U. S. A.* **99,** 13765–70 (2002).

66. Gascoyne, P. R. C., Noshari, J., Anderson, T. J. & Becker, F. F. Isolation of rare cells from cell mixtures by dielectrophoresis. *Electrophoresis* **30,** 1388–98 (2009).

67. Mittal, S., Wong, I. Y., Deen, W. M. & Toner, M. Antibody-functionalized fluid-permeable surfaces for rolling cell capture at high flow rates. *Biophys. J.* **102,** 721–30 (2012).